Ecological Research Series

COOLING TOWER PLUME MODEL

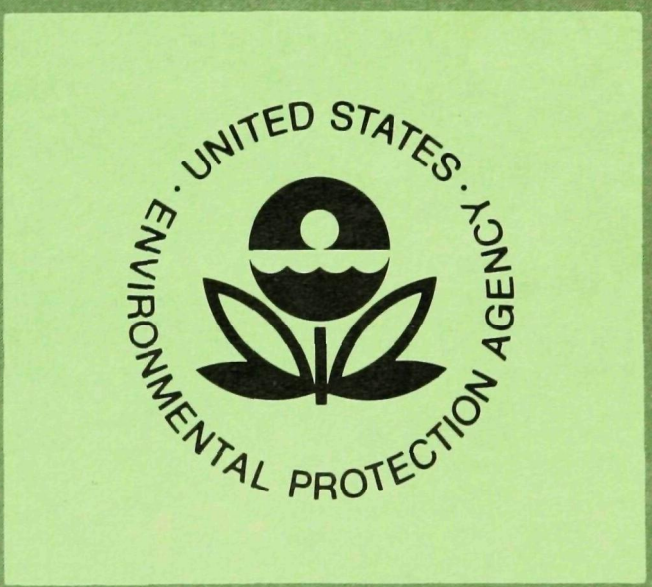

Environmental Research Laboratory
Office of Research and Development
U.S. Environmental Protection Agency
Corvallis, Oregon 97330

RESEARCH REPORTING SERIES

Research reports of the Office of Research and Development, U.S. Environmental Protection Agency, have been grouped into five series. These five broad categories were established to facilitate further development and application of environmental technology. Elimination of traditional grouping was consciously planned to foster technology transfer and a maximum interface in related fields. The five series are:

1. Environmental Health Effects Research
2. Environmental Protection Technology
3. Ecological Research
4. Environmental Monitoring
5. Socioeconomic Environmental Studies

This report has been assigned to the ECOLOGICAL RESEARCH series. This series describes research on the effects of pollution on humans, plant and animal species, and materials. Problems are assessed for their long- and short-term influences. Investigations include formation, transport, and pathway studies to determine the fate of pollutants and their effects. This work provides the technical basis for setting standards to minimize undesirable changes in living organisms in the aquatic, terrestrial, and atmospheric environments.

This document is available to the public through the National Technical Information Service, Springfield, Virginia 22161.

EPA-600/3-76-100
September 1976

COOLING TOWER PLUME MODEL

by

Lawrence D. Winiarski and Walter F. Frick
Assessment and Criteria Development Division
Corvallis Environmental Research Laboratory
Corvallis, Oregon 97330

CORVALLIS ENVIRONMENTAL RESEARCH LABORATORY
OFFICE OF RESEARCH AND DEVELOPMENT
U.S. ENVIRONMENTAL PROTECTION AGENCY
CORVALLIS, OREGON 97330

DISCLAIMER

This report has been reviewed by the Corvallis Environmental Research Laboratory, U.S. Environmental Protection Agency, and approved for publication. Mention of trade names or commercial products does not constitute endorsement or recommendation for use.

FOREWORD

Effective regulatory and enforcement actions by the Environmental Protection Agency would be virtually impossible without sound scientific data on pollutants and their impact on environmental stability and human health. Responsibility for building this data base has been assigned to EPA's Office of Research and Development and its 15 major field installations, one of which is the Corvallis Environmental Research Laboratory.

The primary mission of the Corvallis laboratory is research on the effects of environmental pollutants on terrestrial, freshwater, and marine ecosystems; the behavior, effects and control of pollutants in lake systems; and the development of predictive models on the movement of pollutants in the biosphere.

This report describes the development of a model for predicting cooling tower plumes and the comparison of the model predictions with laboratory and field data.

A. F. Bartsch
Director
Corvallis Environmental Research
Laboratory

ABSTRACT

A review of recently reported cooling tower plume models yields none that is universally accepted. The entrainment and drag mechanisms and the effect of moisture on the plume trajectory are phenomena which are treated differently by various investigators. In order to better understand these phenomena, a simple numerical scheme is developed which can readily be used to evaluate different entrainment and drag assumptions. Preliminary results indicate that in moderate winds most of the entrainment due to wind can be accounted for by the direct impingement of the wind on the plume path. Initially, the pressure difference across the plume is found to produce a substantial drag force. Thus, it is likely that a certain portion of the plume bending is due to these pressure forces, and artificially increasing wind entrainment to fit experimental data is unnecessary.

This report is submitted by the Pacific Northwest Environmental Research Laboratory of the Environmental Protection Agency. Work was completed as of February 1975.

CONTENTS

FIGURES

ACKNOWLEDGEMENT

The assistance, advice and consultation supplied by Mr. James Chasse is gratefully acknowledged.

SECTION I

INTRODUCTION

This report will describe an approach to cooling tower plume modeling which gives predictions which compare favorably to data without requiring specific adjustment of empirical coefficients.

Using basic principles, the fundamental conservation laws are applied to a finite parcel of a cooling tower plume in such a way that it is not necessary to solve simultaneous partial differential equations. Rather, the basic physics can be applied using average properties at a plume cross section. The result is simple algebraic equations that can quickly be solved step by step on a computer. This approach enables one to follow more closely the effect of different entrainment and drag hypotheses. Based upon numerical experiments with this model, a logical physical formulation for the entrainment and drag mechanisms was found which yielded reasonable agreement with laboratory and field data.

Prior to discussion the details of the computational procedure, the following questions are answered.

1. What is meant by a cooling tower plume?
2. What environmental problems are associated with cooling tower plumes?
3. What parameters are required for making plume predictions?
4. What are the basic physical principles and how are they applied in the model?

Following this, the computational procedure of the model can be easily explained because of its close correlation with the physical principles. Finally, a comparison of model predictions with data are given.

The appendix includes a brief technical review of recent plume models, including discussions of the similarities and differences among various models.

In recent years there has been an increasing concern about the potential environmental effects of large cooling tower plumes. These cooling tower plumes consist largely of heated air and water vapor. The water vapor may condense into small droplets, and these pure water droplets form a fog making part of the plume visible. In addition to the condensed water droplets, there is a small amount of circulating water which is carried over with the air rushing through the tower. This water is called drift and has about the same chemical composition as the cooling water in the tower. The visible plume from the cooling tower is chiefly pure water which generally should not be considered harmful. However,

there is reason for concern if the cooling tower plume reduces visibility or contributes to icing at a nearby highway or airport. Drift water could also be a contributing factor to local icing but currently there is also concern about the adverse effects of materials carried with the drift. For example, if seawater is used in the tower the salt deposition might harm nearby vegetation. Chemicals used to control fouling or inhibit corrosion also might be objectionable when spread with the drift. If contaminated water is used, the possibility of spreading bacteria or virus with the drift should be considered. Finally, the question has been raised as to whether cooling towers can affect the weather due to the large releases of both heat and water vapor.

As the questions concerning the possible effects of cooling towers become more detailed, it is desirable to have acceptable mathematical models that have sufficient generality to handle a wide range of possible conditions. A sensitivity analysis with such mathematical models will indicate how carefully one must specify input conditions (ambient meteorology and tower performance) in order to get certain details about cooling tower plumes. There is a possibility that a knowledge of the sensitivity of the plume behavior with respect to input conditions might indicate which environmental questions would warrant most careful consideration and which are not likely problem areas at a given site.

SECTION II

CONCLUSIONS

A numerical model for a cooling tower plume was developed and used to evaluate various entrainment assumptions. It was found that most of the plume bending is due to the momentum of the wind mass that passes through the projected area of the plume. The momentum of the wind mass is imparted to the plume in two ways: (1) The mass entrained gives its momentum directly to the plume; (2) The deflection of some of the wind yields a strong horizontal pressure force near the source. Furthermore, the vertical acceleration of a plume parcel due to buoyant forces must take into account the mass of the wind that has to be displaced.

An entrainment and drag hypothesis was developed that gives reasonable agreement with actual field test data and with laboratory test data for air and water plumes over a wide range of conditions without having to adjust empirical coefficients.

The model is believed to accurately predict average plume properties which are internally consistent and in agreement with fundamental conservation laws.

SECTION III

RECOMMENDATIONS

The entrainment and drag hypotheses developed here should be checked with more detailed data, including a better measure of plume properties over the plume cross section. The basic single cell model should be modified so that it can predict a non-circular cross section. There is some laboratory evidence to indicate that this may occur. Preliminary modifications of the model to predict non-circular cross sections indicate that the model has reached a level of development where this effect can be noticable. More data could also be acquired on multicell towers with the wind coming at various angles to the tower axis. This would aid in understanding the entrainment and drag mechanism for multiple sources. The model should be adapted to handle this situation.

SECTION IV

PERTINENT PARAMETERS

Parameters that must be specified in order to predict plume behavior are:

A. Source parameters

1. Air flow rate
   a. Diameter of tower
   b. Air velocity
2. Temperature
3. Humidity
4. Mass of condensed water (i.e. fog droplets formed inside cooling tower)
5. Drift
   a. Total drift emission
   b. Size distribution

B. Ambient meteorological conditions (variation with altitude)

1. Wind speed
2. Wind direction
3. Temperature
4. Humidity

SECTION V

BASIC PLUME PRINCIPLES

In order to be able to predict plume behavior with any degree of confidence, one must have a good understanding of certain basic phenomena. These phenomena are as follows:

1. Momentum transfer from the wind to the plume.
2. Entrainment or dilution of plume properties due to mixing of ambient air.
3. Buoyancy acceleration.
4. Moisture effects.

MOMENTUM TRANSFER

The wind can impart horizontal momentum to a plume in two ways:

1. By direct entrainment.
2. By pressure differences (drag hypothesis).

It has not been determined how much momentum transfer is due to each mechanism. There is no consensus about either the formulation of the terms or the coefficients. Some (e.g. 13, 15) maintain that all plume bending is due to entrainment of the wind particles by the plume. This results in essentially the inelastic collision problem exemplified in basic physics. (See Figure 1).

It is important to distinguish plume bending due to entrainment from plume bending due to pressure. Numerical experiments were performed which indicate that the amount of entrainment necessary to achieve observable plume bending by entrainment alone would result in excessive dilution of plume properties.

Based on these numerical experiments, it is the hypothesis of this report that the transfer of horizontal momentum from the wind to the plume (thus causing the plume bending) results primarily from the momentum of the wind that passes through the projected area of the plume. (See Figure 2). The mass going through this area imparts its momentum to the plume in two ways. Close to the source, most of the mass is deflected around the jet. This results in a strong pressure force. However, a short distance away from the source, the wind mass begins to penetrate the plume thereby adding momentum by direct entrainment. It is still not certain how to divide the momentum transfer between these two mechanisms, but the hypothesis here is that their sum is always equal to the momemtum in the wind mass passing through the projected area of the plume.

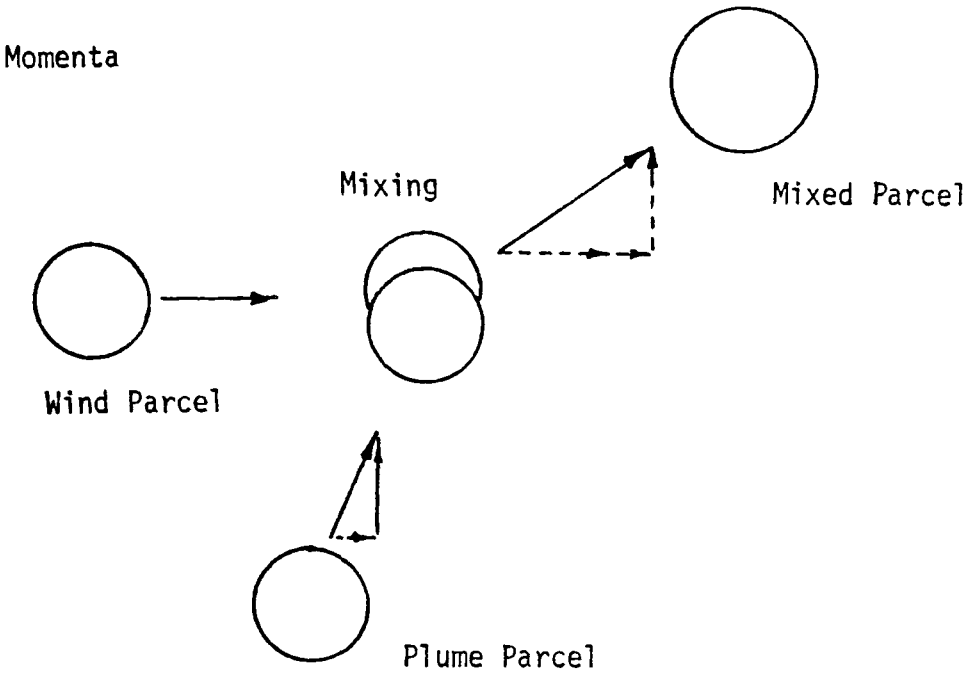

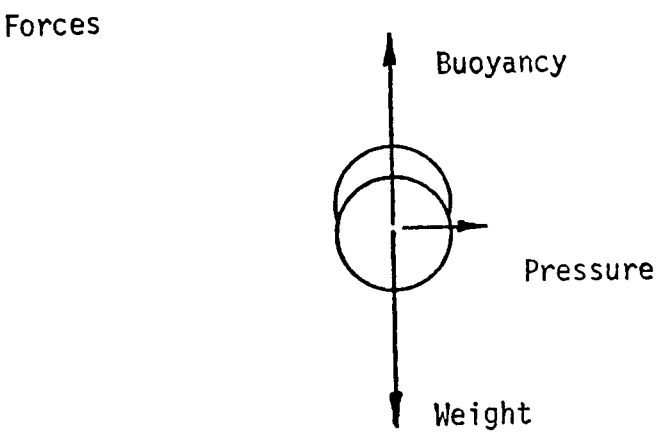

Figure 1. Direction of momenta and forces.

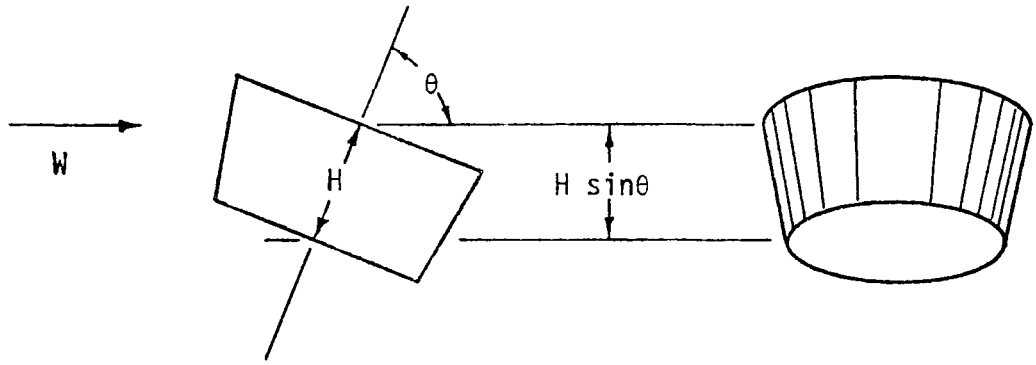

Side view. Front view.

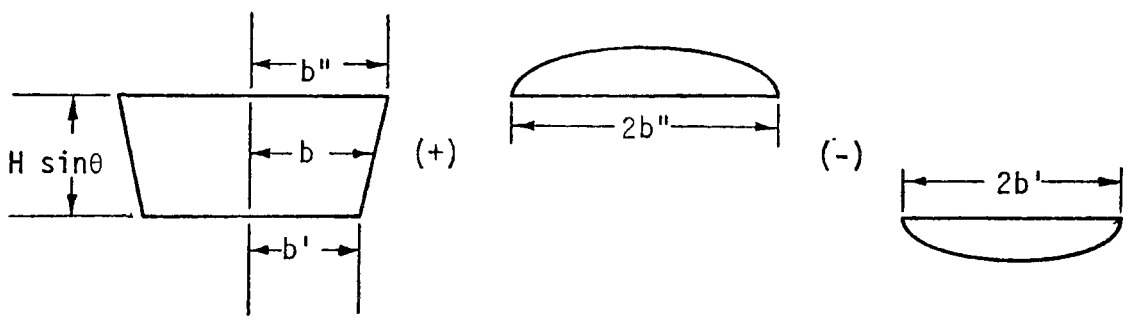

$bH \sin\theta$ $\pi/2\ b''^2 \cos\theta$ $\pi/2\ b'^2 \cos\theta$

$$\text{PROJECTED AREA} = 2bH \sin\theta + (\pi/2)(b''^2 - b'^2) \cos\theta$$

$$= 2bH \sin\theta + (\pi/2)(b'' + b')(b'' - b') \cos\theta$$

$$= 2bH \sin\theta + \pi \Delta b\ b \cos\theta$$

Figure 2. Projected area of plume element.

The plume also induces some mass to be entrained due to the difference between the plume velocity and the wind speed. This can be visualized as an aspiration or shear type entrainment. (See Figure 3). When there is no wind this is the only entrainment. It is not certain how much momentum this aspirated mass adds to the plume. The hypothesis to be used here is that on the average this aspirated mass has a horizontal velocity component equal to the free stream velocity. Generally, the momentum entrained by this mechanism will be less than the momentum entrained by the wind.

ENTRAINMENT

In any detailed calculation of plume behavior, a knowledge of how the plume takes in or mixes with ambient air is critical. However, as is pointed out by Lin (20), the various entrainment mechanisms that have been proposed make it immediately apparent that there is still no consensus regarding the nature of the entrainment mechanism or the correct formulation for the jet trajectory.

It is difficult to compare entrainment and drag coefficients used in different models because the formulation of the entrainment terms are different. Generally, the entrainment term involves the product of an entrainment coefficient and some "characteristic velocity". However, there is no general agreement on what velocity is appropriate. For example, Keffer and Baines (18) assume an entrainment mechanism based upon the scalar difference between the averaged velocity taken over the jet cross-section and the external stream velocity. Their experimental results show the entrainment coefficient to be a variable along the jet trajectory.

In order to account for entrainment due to the pair of vortices in the wake of a jet, Platten and Keffer (23) introduced another entrainment function and therefore another entrainment coefficient.

Fan (9) assumed entrainment mechanics based on the vector sum of the jet velocity and the velocity component of the external stream parallel to the jet trajectory. However, he also included a drag force as though the jet were a solid body.

Hoult, Fay, and Forney (15) assumed two entrainment mechanisms, one due to the difference between the jet velocity and the velocity component of the external stream parallel to the jet trajectory, and the other due to the component of the external stream normal to the jet trajectory. They do not use a drag term.

Hirst (13) uses similar ideas but modifies the first entrainment coefficient so that it is a slight function of Froude number. He does not allow for drag. A tabular comparison of some of the different entrainment and drag formulations is included in the report by Chan and Kennedy (4).

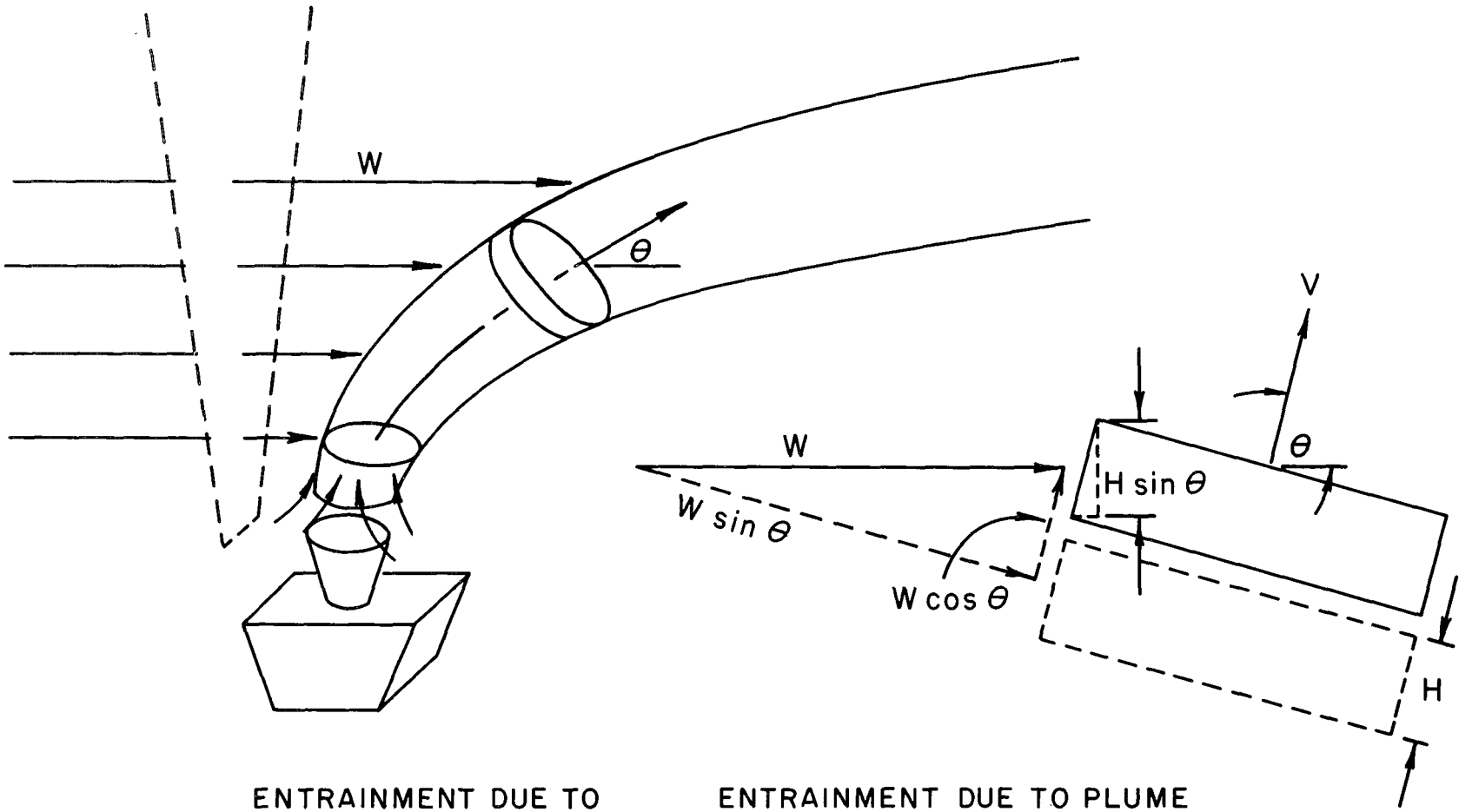

ENTRAINMENT = ENTRAINMENT DUE TO WIND IMPINGEMENT + ENTRAINMENT DUE TO PLUME SEGMENT MOVING WITH VELOCITY RELATIVE TO WIND (ASPIRATION)

$$\rho A_{projected} W \qquad \alpha \rho \pi 2bH|\bar{V} - W\cos\theta|$$

Figure 3 Entrainment mechanisms.

The basic idea of assuming one entrainment mechanism based on the wind component normal to the plume and another based on the difference between the jet velocity and the velocity component of the external stream parallel to the jet trajectory is physically very appealing. (See Figure 3). The parallel shear is like the velocity shear when a jet is discharged into a quiescent media. The coefficient (α) of this self-induced entrainment or aspiration is fairly well established. However, a physical interpretation of the entrainment raises a serious question due to the normal component of the wind.

It is generally assumed (e.g. 4, 13, 15) that the component of the wind normal to the plume is multiplied by the total cylindrical area of the elemental plume surface in order to find the volume entrainment (see Figure 4).

$$W \sin \Theta \, 2\pi b \Delta s \, \beta \tag{1}$$

where β is an entrainment coefficient.

Physically it seems that maximum entrainment due to the direct action of the wind (i.e., not including aspiration) would occur when all of the mass crossing the projected area was mixed with the plume mass and carried up with the plume. This would yield

$$W \, 2b\Delta s \sin \Theta \tag{2}$$

Note that $2b\Delta s \sin \Theta$ is simply the projected area of a cylindrical plume segment in the direction of the wind. If consistent definitions of the plume radius are used it would appear by comparing these relationships that this often used entrainment assumption is too large by the factor $\pi\beta$.

There is evidence to indicate that a large part of the wind impinging on the plume projection tube is actually carried around and entrained in the down wind side of the plume. The wind imparts a double rolling vortex motion to the plume cross section. Chan and Kennedy's data (4) show this to occur near the orifice. An integration of pressure around the plume would imply a drag coefficient.

The hypothesis that will be used in this report is that the aspiration type entrainment can be calculated via the parallel velocity shear (see Figure 3) where the coefficient is assumed ($\alpha \simeq 0.10$). This is similar to several of the models mentioned earlier (e.g. 3, 12). However, the maximum additional mass that can be entrained is simply that which passes through the projected area. Generally, this is less than the maximum because some of the mass passing through the projected area is deflected around the plume and may never enter the plume. Note, however, that a portion of the deflected mass will still be entrained from the back side of the plume by means of the double vortex motion. As mentioned previously, the deflected mass still imparts momentum to the plume, but it does this via the pressure field.

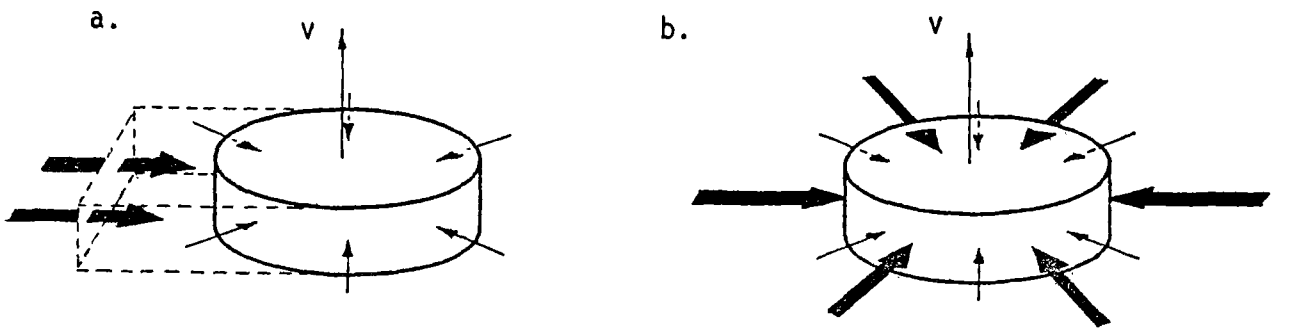

Entrainment

wind	2 p b h w	$\pi \beta$ 2 p b h w = 1.88 (2 p h b w) for a typical β = .6
shear or aspirative	2 α p π b h w	2 α p π b h w

Figure 4. Difference between maximum entrainment assumptions:
a. wind projected area and aspirative entrainment, and
b. effective entrainment due to a typical entrainment assumption.

The reasoning that will be used here is that if the local horizontal pressure force is known or can be estimated, this pressure force can be subtracted from the total horizontal momentum flux to yield the horizontal momentum flux added to the plume by entrainment.

This momentum flux divided by the wind velocity yields the local entrainment. Assuming that the local horizontal pressure force can be approximated as the force needed to decelerate the available mass flux to the velocity of the plume results in the following relationship:

$$\begin{bmatrix}\text{horizontal}\\ \text{pressure}\\ \text{force}\end{bmatrix} = \begin{bmatrix}\text{mass flow}\\ \text{through}\\ \text{projected}\\ \text{area}\end{bmatrix} + \begin{bmatrix}\text{aspirated}\\ \text{mass}\\ \text{flow}\end{bmatrix} \times \begin{bmatrix}\text{wind}\\ \text{velocity}\end{bmatrix} - \begin{bmatrix}\text{horizon-}\\ \text{tal plume}\\ \text{velocity}\end{bmatrix}$$

Finally, after algebraic manipulation, (see Appendix D) there results:

$$\text{Entrainment} = \begin{bmatrix}\text{mass flow}\\ \text{through}\\ \text{projected}\\ \text{area}\end{bmatrix} + \begin{bmatrix}\text{aspirated}\\ \text{mass flow}\end{bmatrix} \times \left[\frac{\text{Horizontal plume velocity}}{\text{wind velocity}}\right]$$

Note that this method of calculation allows for the trends that Chan and Kennedy (4) show in their report. Their data indicates that the initial horizontal pressure force (before a plume parcel has acquired an appreciable horizontal velocity) may be quite large, whereas, the entrainment is initially small, but grows larger. These drag and entrainment hypotheses have been tested using a physical integration scheme that has proved to be simple and direct. A comparison with several data sets is shown in Section 6. Note that there has been no tuning or adjustment of coefficients to match specific data runs. The basic hypotheses in the model account for a variety of conditions.

BUOYANCY

As long as the density of the plume is less than the density of the surrounding air, a net upward force is exerted on the plume parcel. The magnitude of this force can be estimated to be the weight of an equivalent volume of ambient air minus the weight of the plume parcel. This force imparts an acceleration to the plume parcel, but it is not clear how to calculate this acceleration in as much as it is not clear how much mass is involved. It appears that when the plume parcel has a vertical motion into undisturbed ambient air, a mass of ambient air corresponding to the displacement of undisturbed ambient air must be accelerated. In cloud physics work, (7). experiments have also indicated that an equivalent virtual mass must be added to the cloud mass. The virtual acceleration then is the net upward force divided by the total mass involved.

MOISTURE

Moisture affects the plume in several ways:

1. The presence of water vapor in the plume makes it less dense than dry air at the same temperature.

2. If water vapor condenses, latent heat is released. This raises the temperature of the vapor, water and air mixture slightly.

3. Similarly, if liquid water evaporates the temperature of the plume mixture cools slightly.

4. The presence of liquid water (fog drift) increases the average density of the plume mixture.

5. If liquid water falls out of the plume (rain, or drift fall out) the average plume density should decrease.

The calculation of moisture effects is complicated and sensitive to small differences. This is particularly noticeable when both the atmosphere and the plume are close to saturation. In this case, the extent of the visible part of the plume is very sensitive to the ambient humidity.

In attempting to analyze moisture effects a compromise must generally be made between computation time and accuracy. The method which will be used for evaluating moisture effects is shown in the appendix.

SECTION VI

MODEL DEVELOPMENT

The calculation procedure is extremely simple. The trajectory of a group of plume particles (a plume puff) is traced in time. Hence, the method could be basically classified as a Lagrangian formulation. The plume puff gains mass as ambient fluid is entrained and mixed within it, but once entrained the new mass becomes an indistinguishable part of the plume puff. In the simplest version, the plume is assumed to be essentially a cylindrical segment whose radius grows as mass is entrained.

The initial plume mass is identified as the mass issuing from the tower with radius b_o.

$$M_o = \rho \pi b_o^2 H_o \tag{3}$$

H_o is the length of the plume mass and is chosen to be comparable to b_o.

$$H_o = V_o \Delta t \tag{4}$$

The increment in the plume mass is evaluated from the assumed rate of entrainment:

$$DM = \sum_i (\text{rate of entrainment})_i \, \Delta t \tag{5}$$

For instance, assuming the total entrainment is a function of the horizontal wind and a shearing action of the plume relative to the wind as mentioned earlier:

$$DM \simeq \frac{U}{W} \{\rho_{atm} \underbrace{(2bH \sin\Theta + \pi b \Delta b \cos\Theta) W \Delta t}_{\text{approximate project area}} + \underbrace{\alpha \pi 2bH \rho_{atm} |\bar{V} - W \cos\Theta|}_{\text{shear entrainment}} \} \Delta t \tag{6}$$

where an estimate for Δb is $\frac{\partial b}{\partial s} H$, or

$$\Delta b \simeq \frac{(b^t - b^{t-\Delta t}) H}{\sqrt{\Delta x^2 + \Delta z^2}} \tag{7}$$

The values of α in the literature depend on how the plume width, and characteristic velocity are defined and whether the jet is buoyant. The order of magnitude is known but further refinements might be made relative to the particular model. As a first approximation α may be taken to be $\simeq 0.10$ based on experimental studies of submerged jet, (4, 13).

The new horizontal momentum of the plume is simply the old horizontal momentum + the horizontal momentum of the entrained mass + impulse of horizontal pressure (i.e., drag) forces on the plume. The new horizontal velocity (U) of the plume is simply the new horizontal momentum divided by the new plume mass.

$$U^{t+\Delta t} = \frac{M^t U^t + DM \cdot U_w + \text{horizontal pressure force} \times \Delta t}{M^t + DM} \tag{8}$$

Using the momentum hypothesis discussed earlier, the equation for the horizontal velocity can be written without explicitly defining the horizontal pressure as:

$$U^{t+\Delta t} = (M^t U^t + \rho_{atm}(2bH \sin\Theta + \pi bdb \cos\Theta) W^2 \Delta t \tag{9}$$
$$+\alpha \rho_{atm} \pi 2bH|\bar{V}-W \cos\Theta|W\Delta t)/(M^t+DM)$$

Note, however, that the assumption for the horizontal pressure force from which the particular entrainment hypothesis was derived is:

$$\text{Horizontal pressure force} = (\rho_{atm}(2bH \sin\Theta + \pi bdb \cos\Theta) W + \alpha\rho_{atm} \pi 2bH|V-W \cos\Theta|)(W-U) \tag{10}$$

Assuming the total pressure force vector acts normal to the plume it is possible to approximate a vertical pressure force component (provided the plume is not close to horizontal) as:

$$\text{Vertical pressure force} \simeq -\frac{\text{horizontal pressure force}}{\tan\Theta}$$

Physically this term tends to zero as $\tan\Theta$ tends to zero but because of the numerical treatment this term has to be set to zero; in this case it is set to zero when $\tan\Theta = 0.1$.

Similarly, the new vertical velocity due to entrainment is:

$$V^{t+\Delta t} = \frac{M^t V^t + (\text{vertical pressure force})\,\Delta t}{M^t + DM} \tag{11}$$

Note that for a horizontal wind, the entrained mass does not carry any vertical momentum with it.

The new plume mass is:

$$M^{t+\Delta t} = M^{t} + DM \tag{12}$$

The new plume temperature is:

$$T^{t+\Delta t} = \frac{M^{t}T + DM\ T_{atm}}{M^{t}+DM} - (\text{ambient lapse})\ \Delta Z \tag{13}$$

The new plume density is evaluated from an equation of state

$$\text{e.g.,} \qquad \rho = \frac{P}{RT} \tag{14}$$

The inclusion of concentrations of other parameters such as water vapor, water droplets, salt drift, etc., requires slight modifications in the temperature and density calculations, but the basic philosophy is the same. A routine for calculating phase change is explained in Appendix II.

The change in the density of the plume relative to the atmosphere results in a buoyant force imparting a vertical acceleration to the plume mass equal to:

$$a \simeq \frac{\rho_{atm} - \rho_{plume}}{2\ \rho_{plume}}\ g \tag{15}$$

This vertical acceleration modifies the new vertical velocity by

$$\Delta V = a\ \Delta t \tag{16}$$

Therefore:

$$V^{t+\Delta t} = V^{t+\Delta t} + \Delta V \tag{17}$$

The new location (trajectory of the plume puff) is:

$$X^{t+\Delta t} = X^{t} + \frac{U^{t} + U^{t+\Delta t}}{2}\ \Delta t \tag{18}$$

$$Z^{t+\Delta t} = Z^t + \frac{V^t + V^{t+\Delta t}}{2} \Delta t \tag{19}$$

The speed of the plume puff along the trajectory is:

$$\bar{V} = \sqrt{U^2+V^2} \tag{20}$$

The sine of the angle of inclination is:

$$\sin \Theta = \frac{\bar{V}}{\sqrt{U^2+V^2}} \tag{21}$$

The average radius of the plume puff can be found:

$$\rho \pi b^2 H = M \tag{22}$$

$$b = (M/\rho \pi H)^{1/2}$$

Where the elemental plume puff length H is

$$H^{t+\Delta t} = H^t + \frac{(\bar{V}^t - \bar{V}^{t-\Delta t})}{\sqrt{(dX)^2+(dY)^2}} H^t \Delta t \tag{23}$$

Time is updated

$$t = t+\Delta t \tag{24}$$

and the procedure is repeated. The Lagrangian Puff models for water and air are included in Appendix C.

SECTION VII

COMPARISON WITH DATA

The model predictions have been compared with three different types of data:

1. Laboratory tests with air jets.
2. Actual field data taken on a large single cell cooling tower.
3. Laboratory tests with plumes in water.

A comparison with non-bouyant air jet data is shown in Figure 5. Note that two independent sets of centerline data points are shown. The model centerline predictions, indicated by solid lines, compare closely without having to "tune" any coefficients. The parameter K, shown on Figure 5, is the ratio of exit velocity to wind velocity.

A comparison with actual field data taken by the Environmental Protection Agency using the technique shown in Figure 6 is given in Figures 7a-7g. A lightweight (130 gram) radiosonde transmitter was attached to the tail of an 8-foot long blimp which was tethered to the cooling tower and allowed to "wind vane" downward. The blimp was used in preference to a spherical balloon because it generated aerodynamic lift as the wind increased, and flew much like a kite, rising higher with stronger winds. A tethered spherical balloon would have practically no aerodynamic lift and could be blown close to the ground in a strong wind.

An operator, positioned underneath the balloon, traversed the balloon vertically through the plume by means of a lightweight monofilament line hanging from the balloon (see Figure 6). Simultaneous sightings of the balloon from a theodolite and a transit spaced a known distance apart were correlated with the temperature and humidity recorded by the radiosonde receiving station. The temperature sensor in the radiosonde had a time constant of approximately 2.5 seconds with an accuracy of $\pm$ 0.2°C. The humidity sensor was a premium carbon hygristor with an accuracy of about 5 percent and a time constant similar to the temperature sensor's.

The data plotted in Figures 7a-7g show the temperature and absolute humidity (or mixing ratio), grams of water per kilogram of air, as a function of the height above the ground at a given distance from the tower. The dotted lines show the predicted width, height, average temperature and average absolute humidity for the same conditions. In order to facilitate comparison of the atmospheric gradient (lapse rate) with the adiabatic or neutral gradient, the temperature profile is plotted between parallel lines whose slope is equal to the adiabatic lapse rate (9.8°C/km).

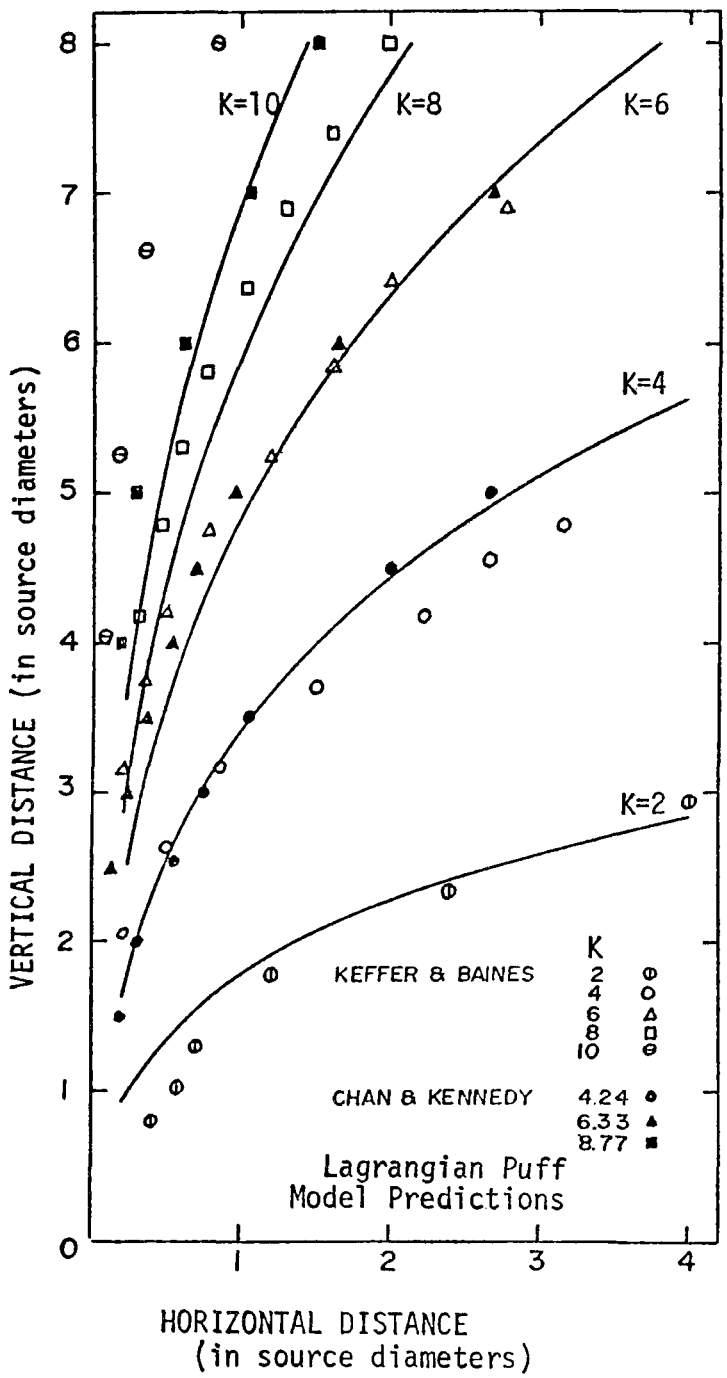

Figure 5. Lagrangian Puff Model predictions compared with jet data.

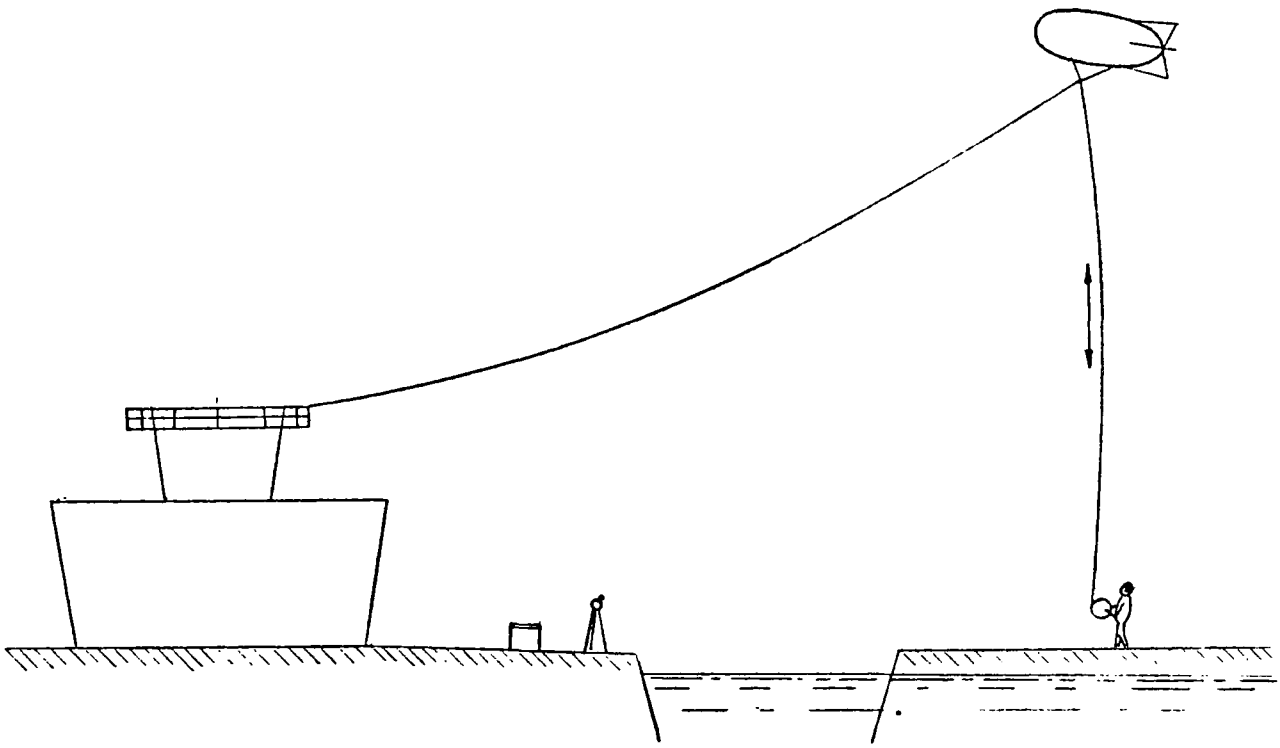

Figure 6. Plume sampling technique.

Relative humidity was the humidity parameter actually measured; however, it was deemed more appropriate to use the temperature data along with the relative humidity data to calculate the actual vapor content. The plume can be discerned better by examining a profile of absolute humidity which, in a well mixed environment, is more nearly uniform. Relative humidity, however, would change with temperature even if the water content is constant. The wind conditions at the site together with the measured lapse rate indicated that for most of the data runs the atmosphere could be considered well mixed.

The data used to plot the curves shown were discrete points tabulated from a strip chart recorder. On the order of 50 data points were used for each run, roughly 10 per minute. The data plotted show the significant fluctuation but not all the fluctuations that were recorded.

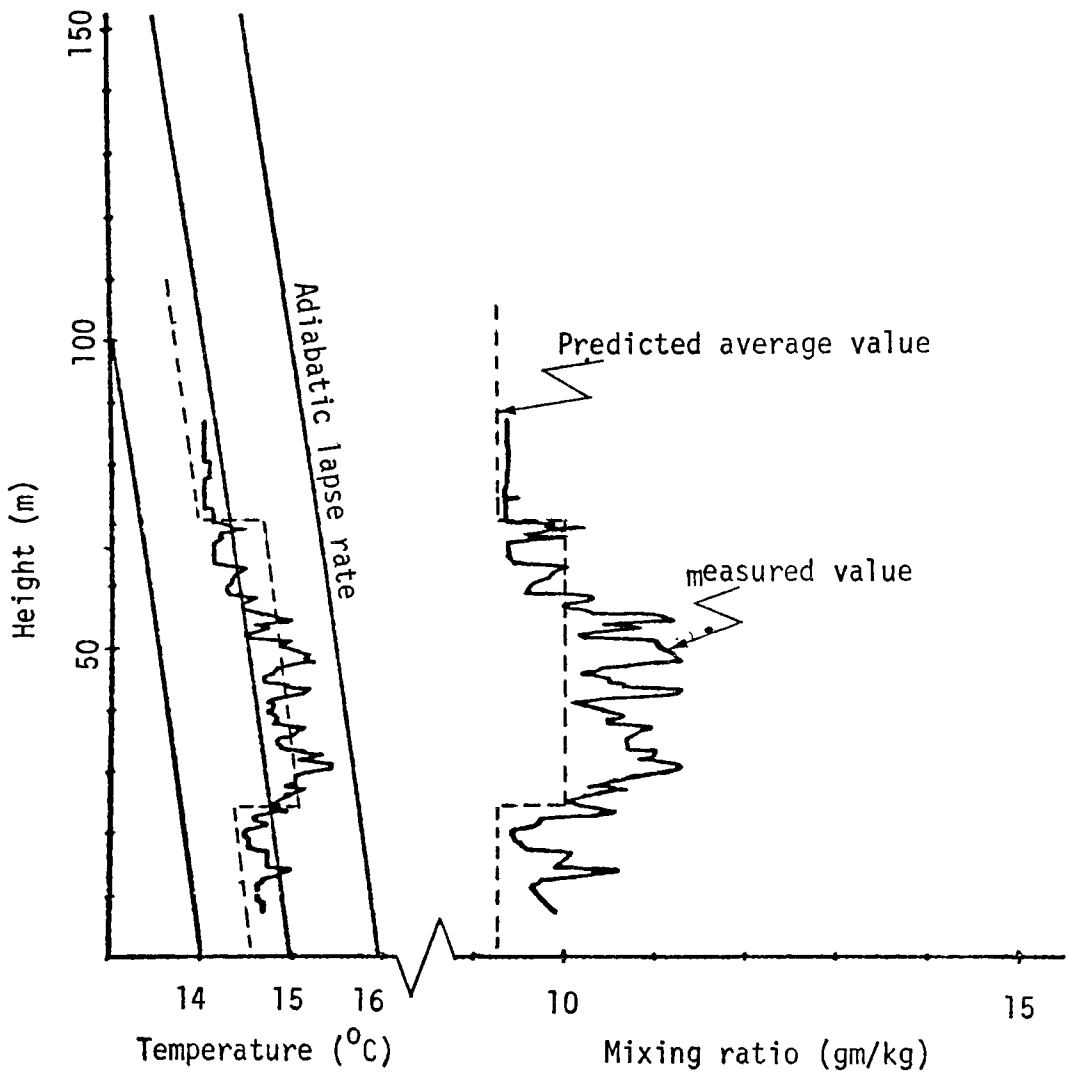

Figure 7a. Cooling tower plume data (Turkey Point) vs. model predictions. Average Runs 1 and 2, 25 Feb 74, 125m horizontal distance. See Table I for input data.

TABLE 1. INPUT CONDITION USED IN FIGURE 7a - 7g

PARAMETERS	7a	7b	7c	7d	7e	7f	7g
Initial temperature °C	30.0	33.2	33.5	30.0	31.1	25.8	25.0
*Efflux velocity m/sec	8.4	8.4	8.4	8.4	8.4	8.4	8.4
Initial liquid water kg/kg	0.0	0.0	0.0	0.0	0.0	0.0	0.0
Source height m	13.0	13.0	13.0	13.0	13.0	13.0	13.0
Source diameter m	8.0	8.0	8.0	8.0	8.0	8.0	8.0
Pressure mb	1000.0	1000.0	1000.0	1000.0	1000.0	1000.0	1000.0
13 m wind (U_w) m/sec	5.4	4.3	3.9	5.4	5.8	7.0	5.9
Wind lapse sec^{-1}	-0.011	-0.033	0.0	0.0	-0.03	0.0	+0.024
13 m temperature °C	14.5	25.3	26.0	17.5	23.2	17.5	15.2
Temperature lapse °C/m	-.009	-.012	-.02	-.012	-.014	-.014	-.015
Ambient mixing ratio kg/kg	0.0093	0.0142	0.0164	0.0094	0.0100	0.0054	0.0067
Source mixing ratio kg/kg	----------	----------	----------	Saturated	----------	----------	----------

*The volumetric air flow, determined by averaging several traverses, was 422 m^3/sec

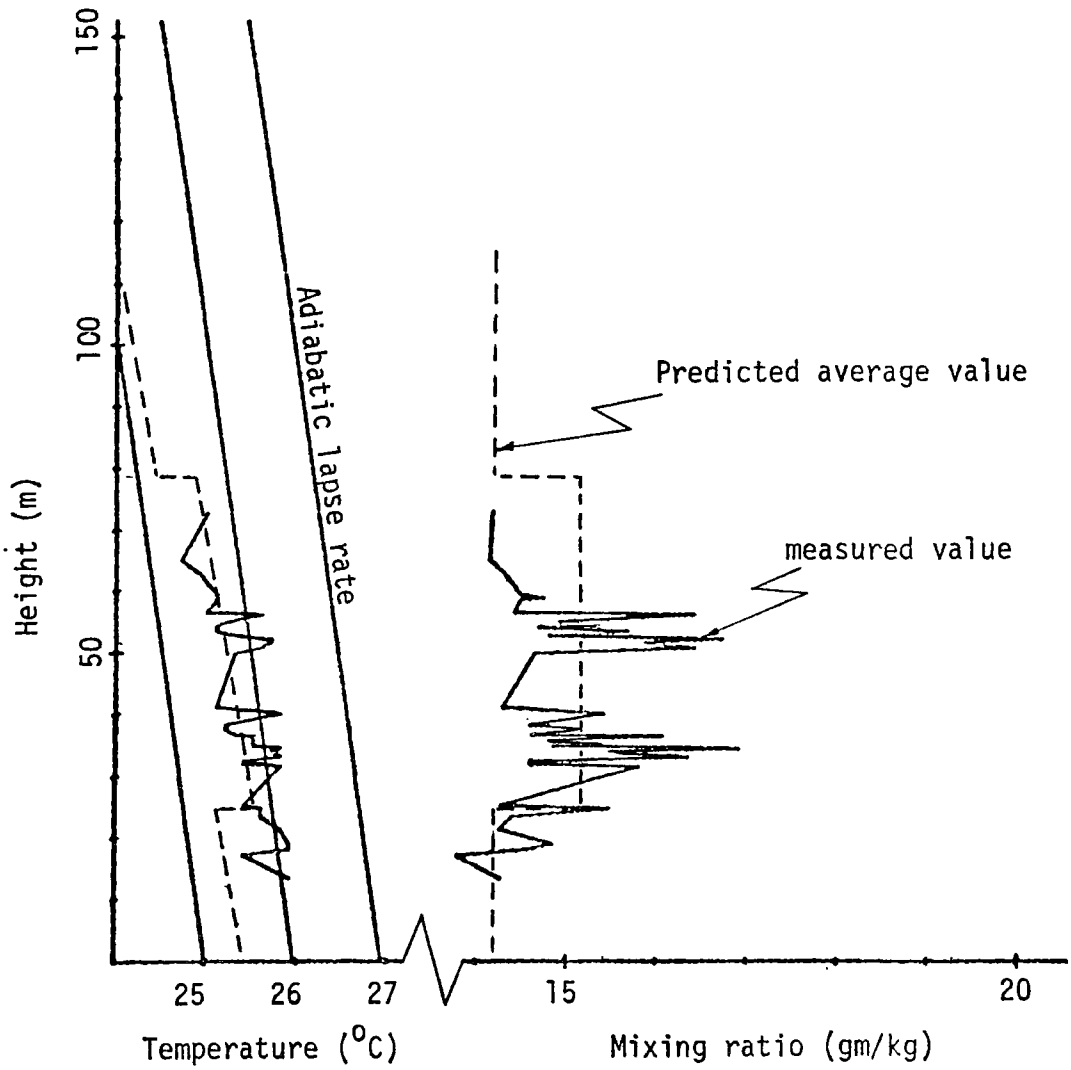

Figure 7b. Run 9, 23 Feb 74, 75m horizontal distance.

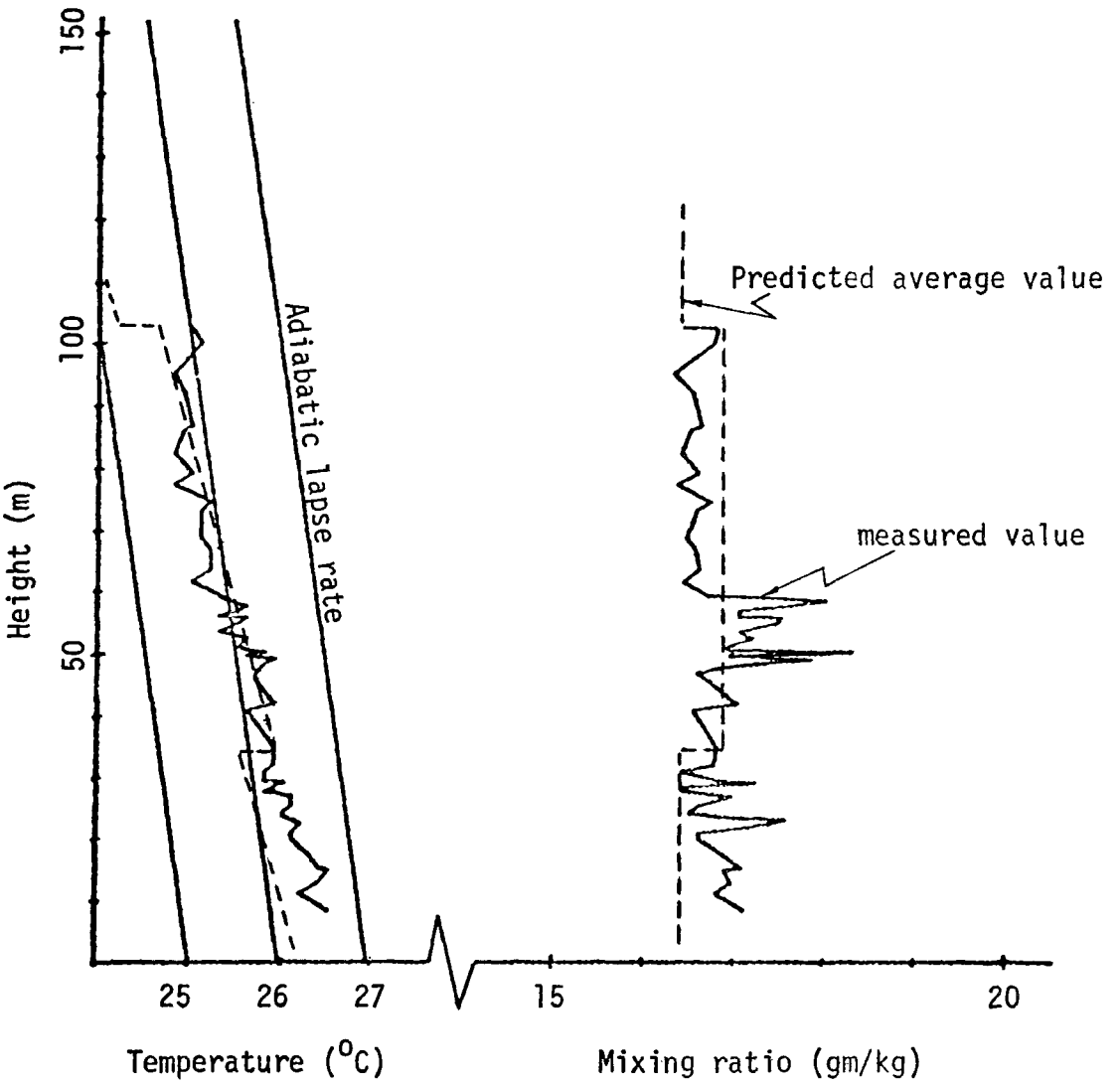

Figure 7c. Run 17, 23 Feb 74, 225m horizontal distance.

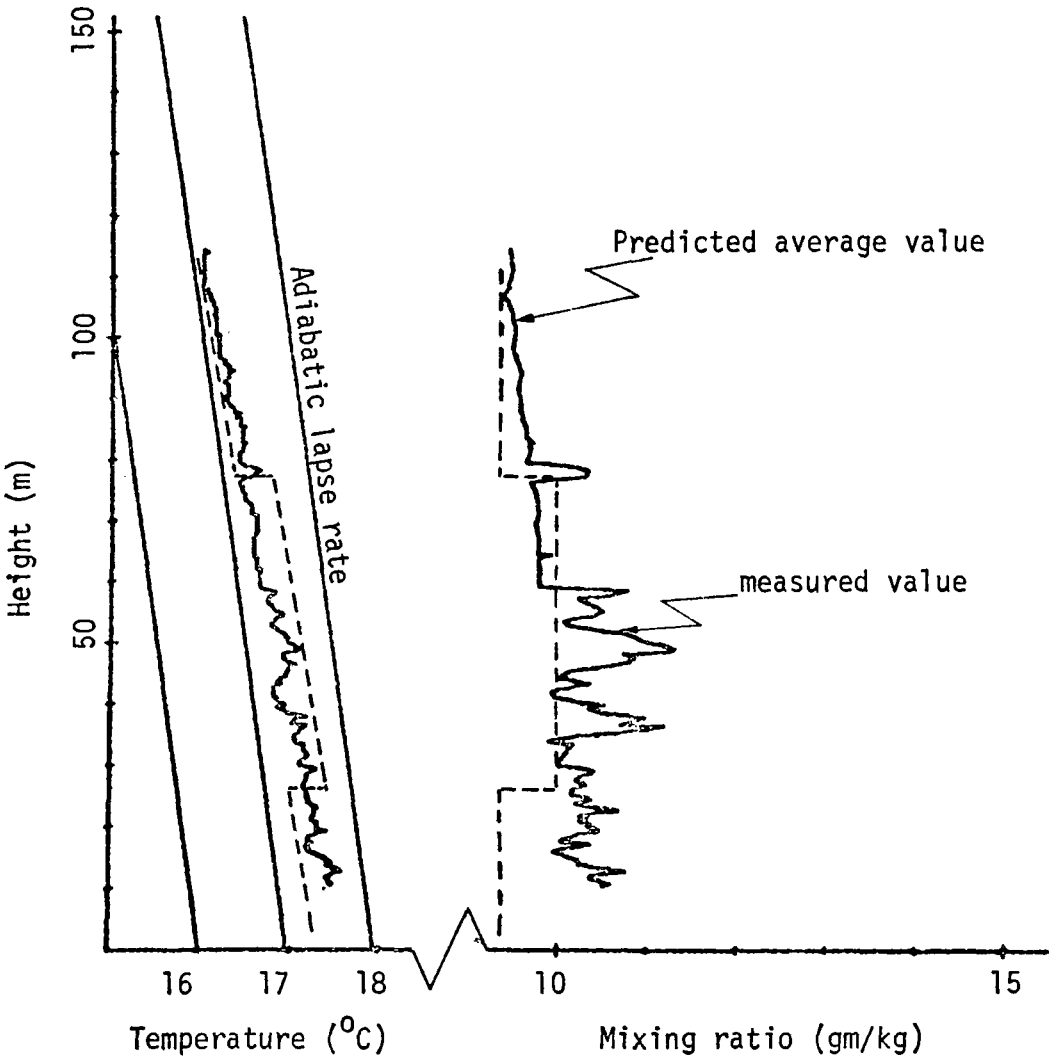

Figure 7d. Average Runs 3,4, and 5, 25 Feb 74, 200m horizontal distance.

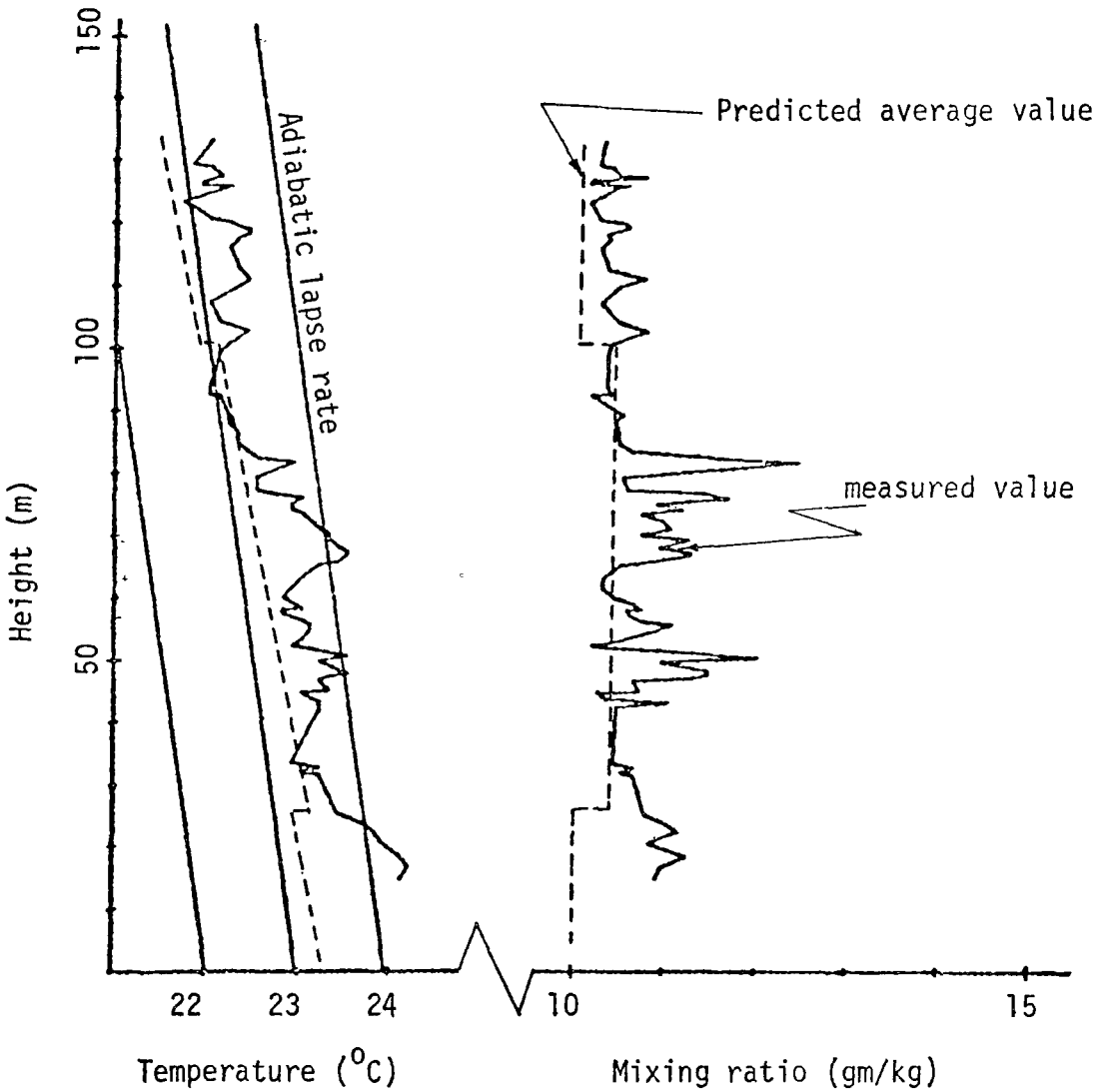

Figure 7e. Run 10, 25 Feb, 240m horizontal distance.

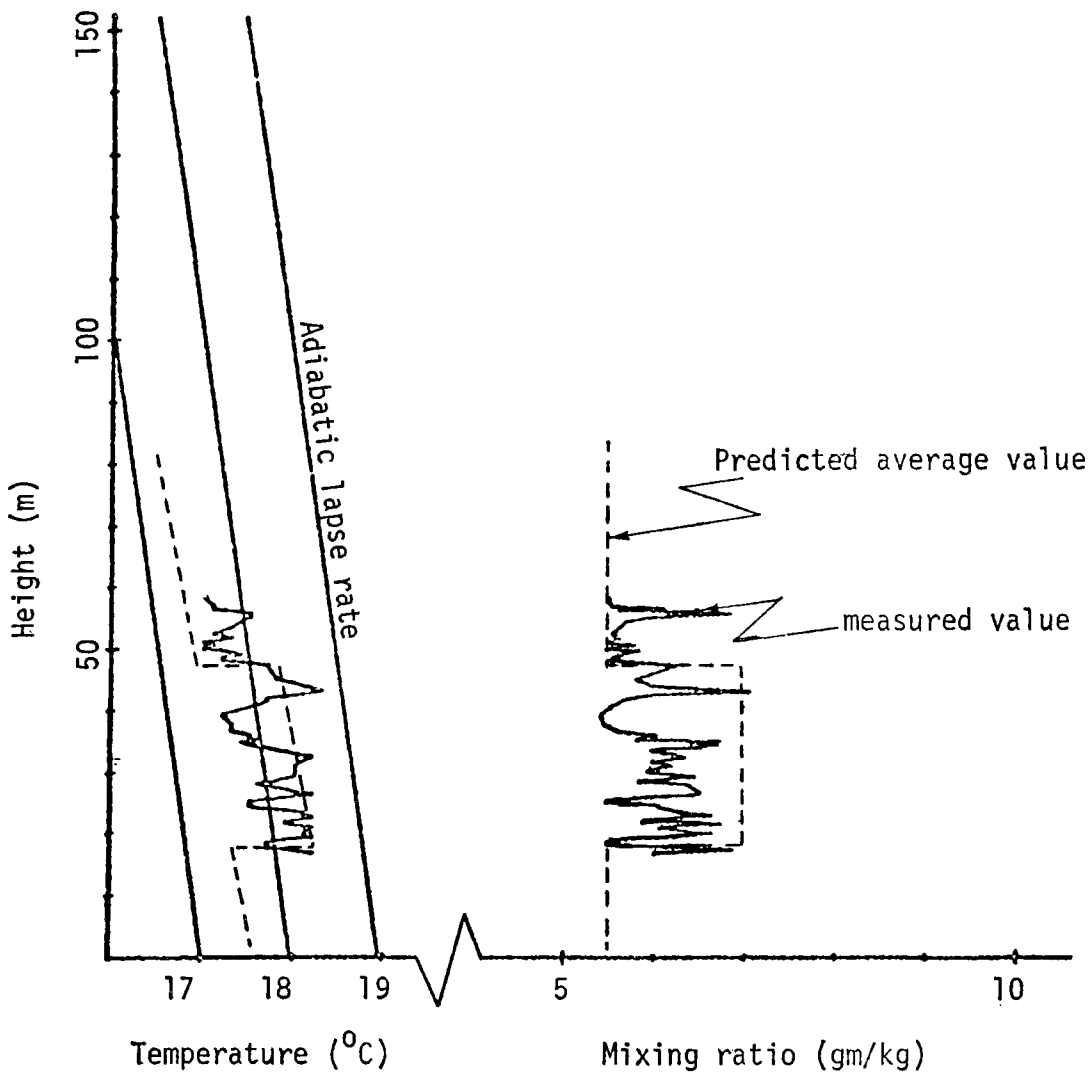

Figure 7f. Run 9, 26 Feb 74, 125m horizontal distance.

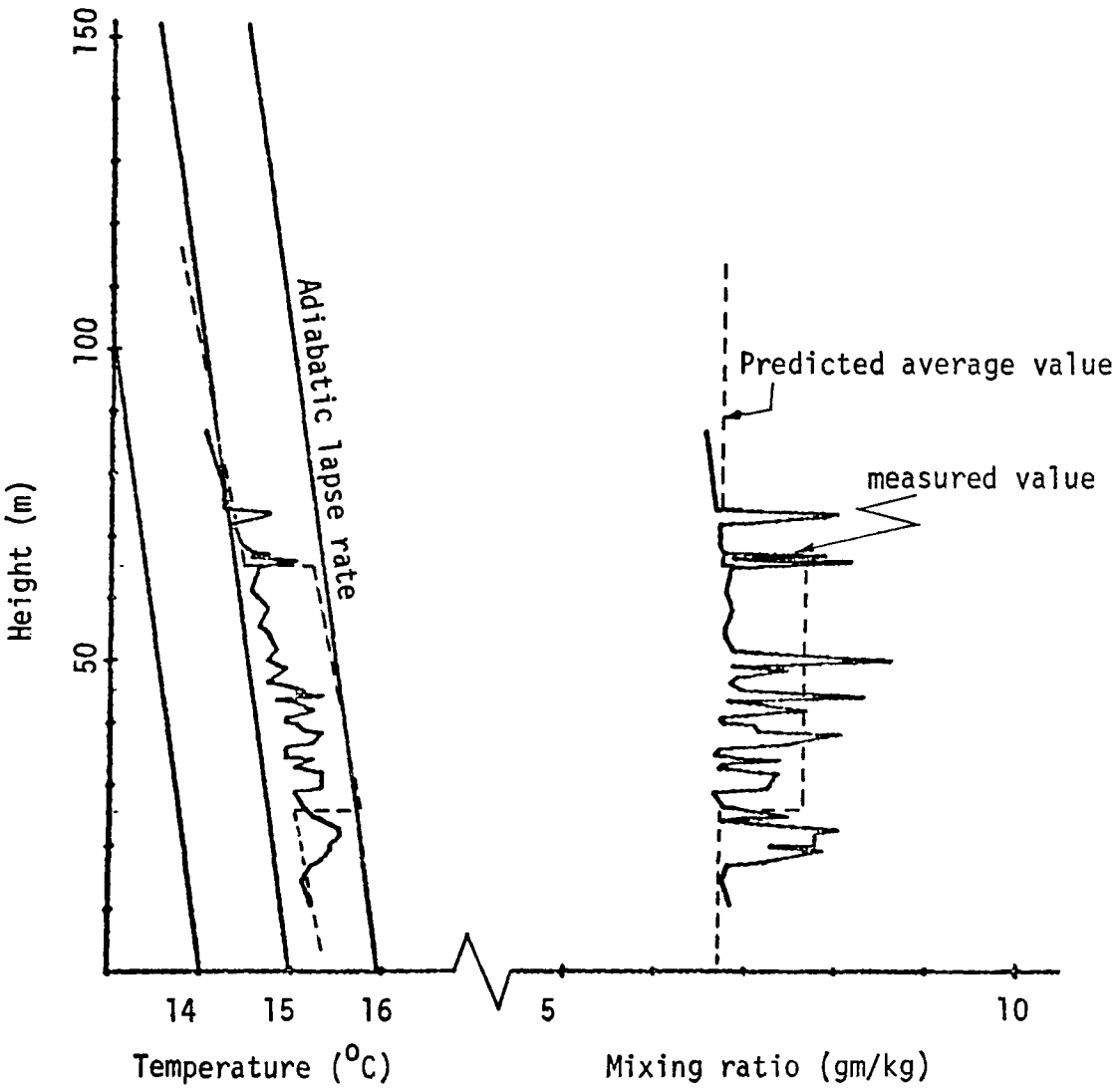

Figure 7g. Run 5, 27 Feb 74, 130m horizontal distance.

Atmospheric conditions were generally fairly steady during the approximately five minutes it took to make a traverse. However, even under these conditions, the plume may exhibit transient behavior. In some cases it is desireable to put together a composite profile by averaging several short-term observations. In Figure 7a the plots are made by averaging together those data runs which were made at the same downwind location under nearly the same environmental conditions. Figure 7a yields the best definition of the invisible plume.

It is desirable to check the model under a variety of conditions. Unfortunately good field data are very scarce and difficult to obtain. Most of the data available are for cases where the wind bends the plume over within a rather short distance. In order to check out a plume model, it is necessary to look at how the model predicts for a wide range of conditions. Figure 8 shows how the model predicts over a range of both velocity and Froude numbers. It is difficult to find a comprehensive set of consistent data to check this range of parameters in order to make such an overall comparison.

The format of Figure 8 facilitates an overall comparison of how different source and ambient conditions affect plume trajectory, temperature and width. The plume trajectories for four different Froude numbers (F = 5, 10, 20, 50) are indicated by the long dashed or solid lines that represent the center lines of the plumes as they bend over in the wind. (The Froude number is the ratio of inertia force to bouyant force, and thus is an inverse measure of bouyancy.) The effect of wind on the plume may be seen by comparing the trajectories for the three different K values shown K = 2, 5, 10. (Recall that K is the ratio of source velocity to wind velocity and hence is an inverse measure of the wind effect). In any given set of K values, isopleths of temperature excess ratios (solid lines) and isopleths of width ratios (short dashed lines) are shown. The ratio of widths is the width of the plume at that point divided by the initial diameter: equal to R/R_o. The temperature ratio excess is the difference between the local average plume temperature and the ambient temperature divided by the difference between the initial average plume temperature and the ambient temperature. The plume temperature always decreases because it is mixing with a cooler environment so the temperature excess ratios are less than one. The values of the temperature excess ratio isopleths and the "width" ratio isopleths are indicated at opposite ends of their respective lines. A small legend indicating the meaning of all the lines is shown in the upper left hand corner of Figure 8.

The curves in Figure 9 have been generated by fitting exponential functions of the dimensionless parameters to Fan's (9) data set, a manner patterned after the analysis by Shirazi et al., (24). This provides a means of interpolating and extrapolating Fan's data for a range of parameters.

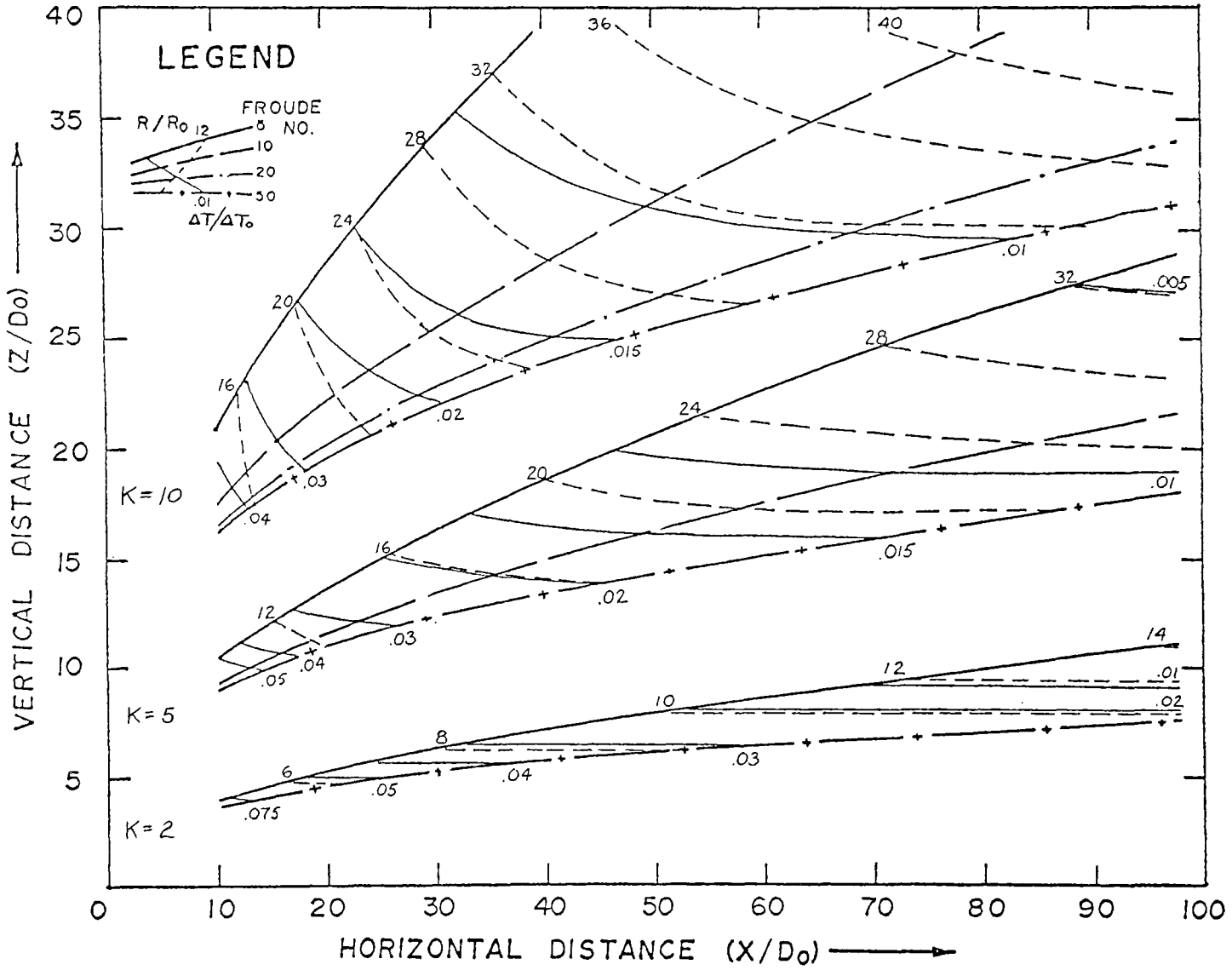

Figure 8. Model predictions of buoyant temperature plume in water.

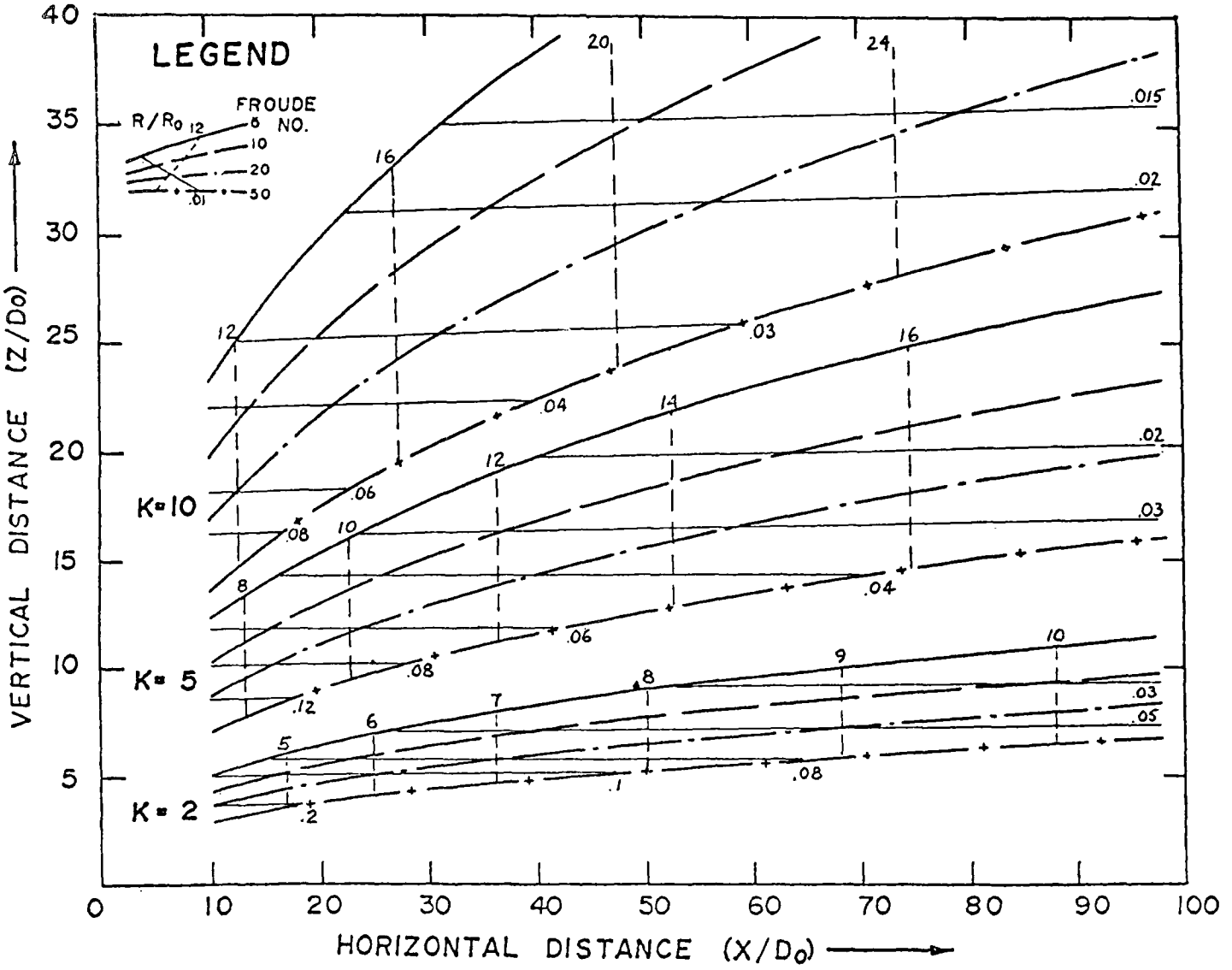

Figure 9. Multiple regression fit to Fan's data (Ref. 6).

A similar set of regression fit curves derived from measurements reported by Chasse and Winiarski (5) is shown in Figure 10. The trajectories of Figure 9 and Figure 10 are roughly similar. Figure 10 was based on temperature measurements whereas Fan's measurements were based on salinity concentrations. The order of magnitude is comparable between Figure 9 and Figure 10. However it should be emphasized that neither Figure 9 nor Figure 10 can be used as an absolute standard in as much as different sets of data yield somewhat different regression fitted curves.

A comparison between the trajectories predicted by the model and the trajectories from the regression fit to Fan's data is shown in Figure 11. With respect to the entire range of parameters shown, the trajectory correlation is reasonable. The differences between the model prediction and the regression fitted trajectories are of the order of the experimental uncertainty of the measurements.

Comparison between the predicted temperature ratios in Figure 8 and the regression fit temperature curves in Figure 9 is more complicated because Fan's temperature data are based on the "peak" temperatures of vertical temperature profiles made through the center of the plume, whereas the predicted temperature ratio in Figure 8 is the average over a plume cross section with finite width. If the average excess temperature were redistributed axisymmetrically with either a linear profile over the same predicted width or a Gaussian profile with the width encompassing about 95 percent of the distribution equal to the predicted width, the peak excess temperature would be about three times the average excess temperature (see Figure 12).

The difficulty in making an absolute comparison is that the plume cross-section and temperature distribution are not always axisymmetric. A few detailed concentration surveys over a complete plume cross-section show that the profile may be double-humped with twin peaks on either side of the centerline. Judging from Fan's (9) cross-sectional isopleths, Figure 13, these off-center peaks can be quite high, sometimes 70 percent greater than the centerline peak. In this particular example, the ratio of the centerline peak excess temperature to the average excess temperature is on the order of two.

In other words, to estimate centerline peak values from Figure 8 to compare with Figure 9 one might multiply the average excess temperature ratio by a factor of 3 if the local cross-section were Gaussian axisymmetric or somewhat lower than 3 were the profile bimodel. Again, the regression fitted curves should not be regarded as absolute values. A regression fit to another data set cf. (Figure 10) show the temperature lines to slope more like that predicted by the model. With these considerations in mind, the predicted temperature ratios are in reasonable agreement with the regression fitted curves.

It is very difficult to try to compare plume "widths" between Figures 8 and 9. The predicted width can best be interpreted as the average radius of a plume cross-section. However, the plume cross-section may sometimes be elliptical or horseshoe-shaped.

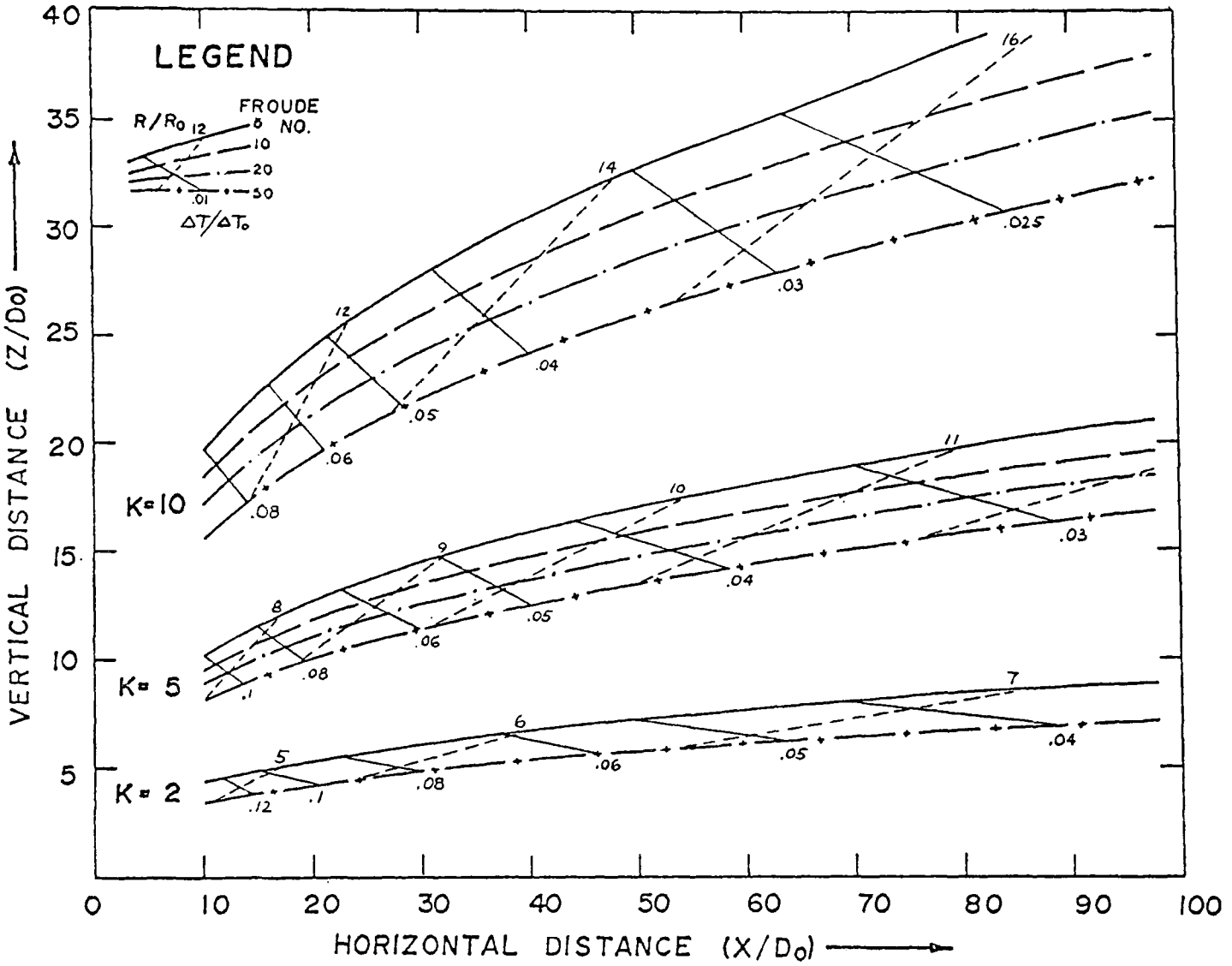

Figure 10. Multiple regression fit to EPA data.

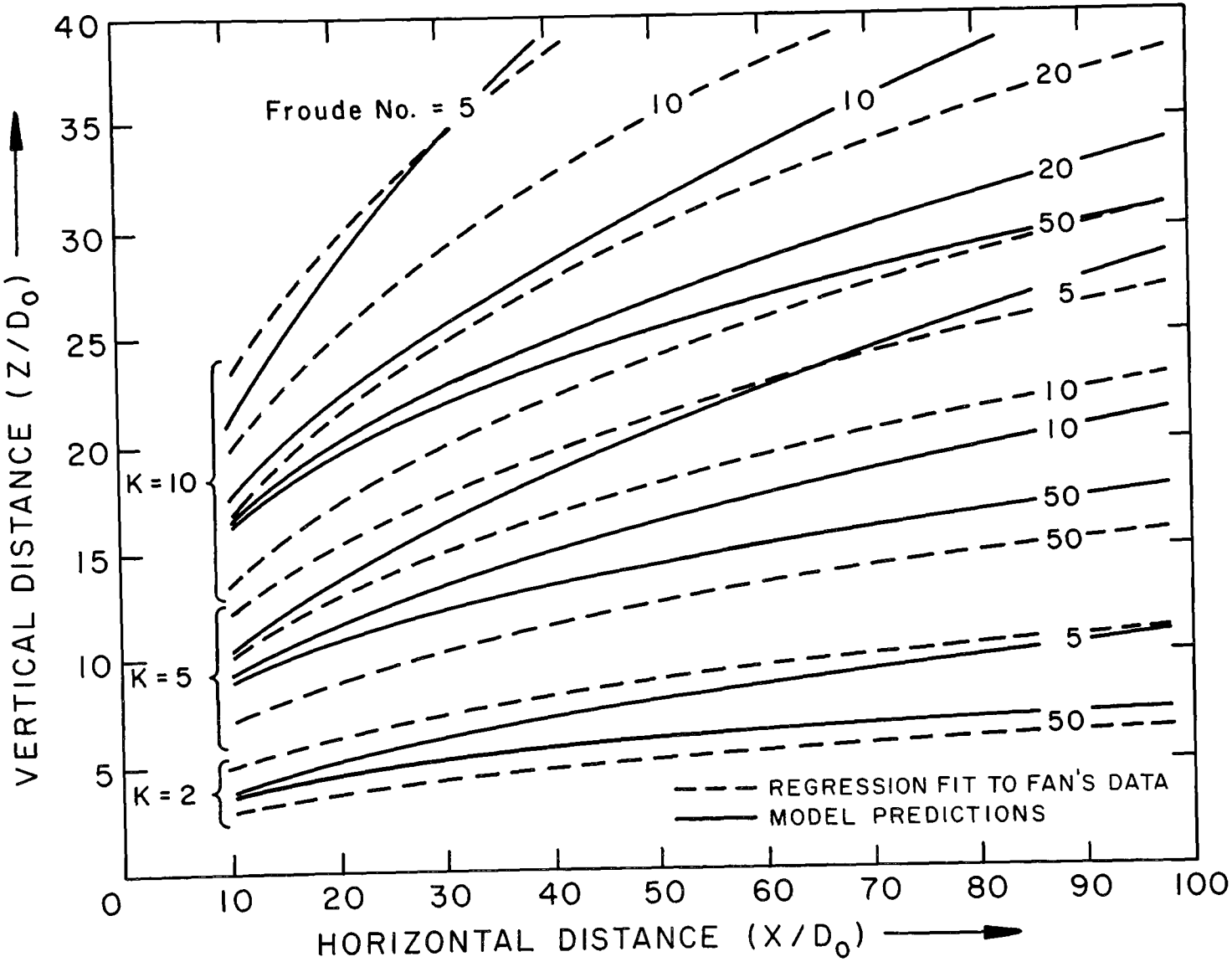

Figure 11. Comparison between model trajectory predictions and regression fit trajectories based on Fan.

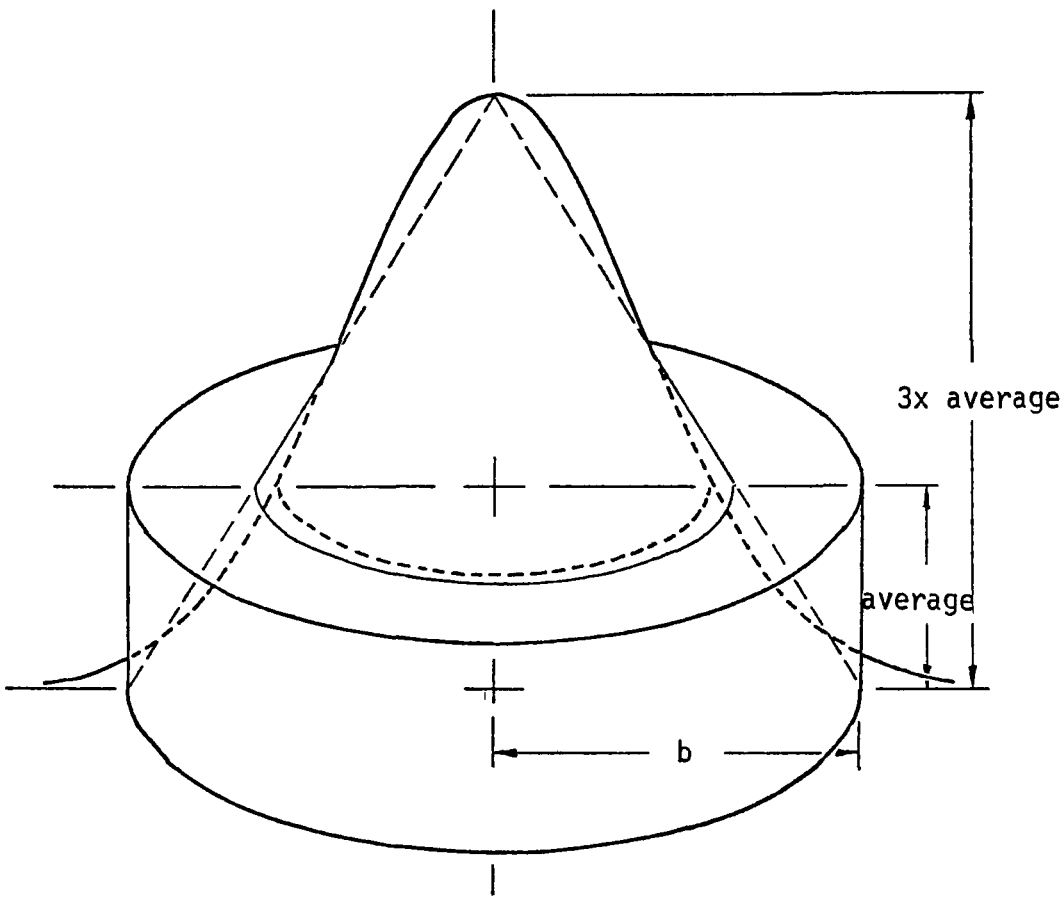

Figure 12. Comparison of Gaussian and linear profiles with average "top hat" value.

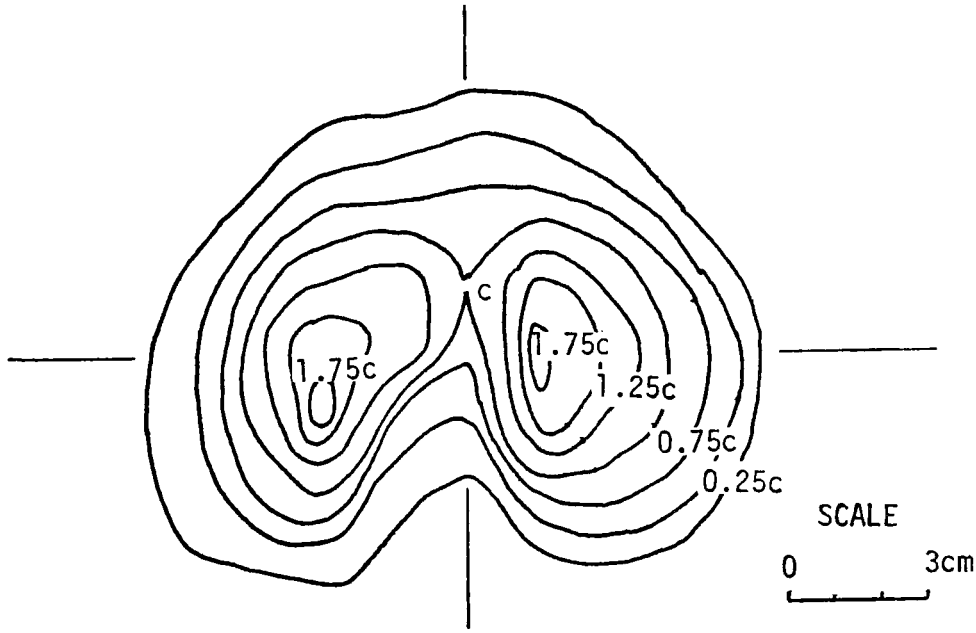

A. Plan view. Zero isopleth is not shown. The centerline peak concentration is (c).

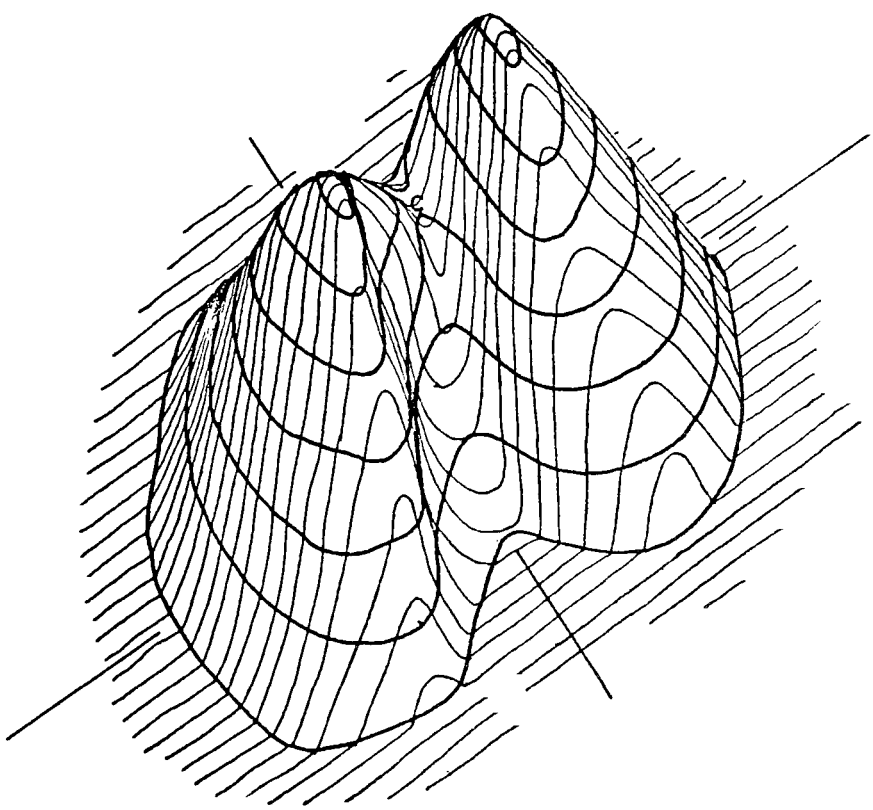

B. Perspective view.

Figure 13. Isopleths of concentration after Fan (Ref: 6).

Furthermore, the half width used in Figure 9 was defined as the width where the concentration was half the centerline peak measurement. Thus, the width curves are not really very comparable. Preliminary modifications to the model which provide a mechanism to allow for the flattening of the plume to an ellipsoidal profile indicate that "width" curves in Figure 8 based on the minor axis would tend to be more nearly vertical. The temperature curves remain about the same, because the average properties which adhere to the fundamental conservation principles remain basically the same.

SECTION VIII

REFERENCES

1. Aynsley, E. and J. E. Carson. Environmental Effects of Water Cooling for Power Plants: A Status Report. Argonne National Laboratory, Argonne, Illinois. Unpublished. 1973.

2. Briggs, G. A. Plume Rise. U. S. Atomic Energy Commission, Oak Ridge, Tennessee. Critical Review Series TID-25075. November 1969.

3. Briggs, G. A. and S. R. Hanna. Comments on a Comparison of Wet and Dry Bent-over Plumes. Journal of Applied Meteorology 11:1386-1387, December 1972.

4. Chan, T. L. and J. F. Kennedy. Turbulent Nonbuoyant or Buoyant Jets Discharged into Flowing or Quiescent Fluids. University of Iowa, Iowa City. Iowa Institute of Hydraulic Research, Report No. 140. August 1972.

5. Chasse, J. P. and L. D. Winiarski. Laboratory Experiments of Submerged Discharges with Current. U. S. Environmental Protection Agency, Corvallis, Oregon. Pacific Northwest Environmental Research Laboratory, Working Paper No. 12. June 1974.

6. Csanady, G. T. Bent-over Vapor Plumes. Journal of Applied Meteorology 10:36-42, February 1971.

7. Davies-Jones, Robert P. Discussion of Measurements Inside High-Speed Thunderstorm Updrafts. Journal of Applied Meteorology 13:710-717, September 1974.

8. EG&G, Inc. Potential Environmental Modifications Produced by Large Evaporative Cooling Tower. Federal Water Quality Administration, Washington, D.C. Report 16130DNH01/71. January 1971.

9. Fan, L. N. Turbulent Buoyant Jets Into Stratified or Flowing Ambient Fluids. California Institute of Technology, Pasadena. W. M. Keck Lab of Hydraulics and Water Resources, Report No. KH-R-15. June 1967.

10. Fay, J. A. M. Escudier, and D. P. Hoult. A Correlation of Field Observations of Plume Rise. Journal of the Air Pollution Control Association 20:391-397, June 1970.

11. Hanna, S. R. Rise and Condensation of Large Cooling Tower Plumes. Journal of Applied Meteorology 11:793-799, August 1972.

12. Hewett, T. A., J. A. Fay, and D. P. Hoult. Laboratory Experiments of Smokestack Plumes in a Stable Atmosphere. Atmospheric Environment 5:767-789, 1971.

13. Hirst, E. A. Analyses of Round, Turbulent Jets Discharged to Flowing Stratified Ambients. Oak Ridge National Laboratory, Oak Ridge, Tennessee. Report ORNL-4685. June 1971.

14. Hosler, C. L. Wet Cooling Tower Plume Behavior. Presented at American Institute of Chemical Engineering 68th National Meeting, Houston, Texas. March 2, 1971.

15. Hoult D. P., J. A. Fay and L. J. Forney. A Theory of Plume Rise Compared with Field Observations. Journal of the Air Pollution Control Association 19:585-590, 1969.

16. Hoult, D. P. and J. C. Weil. Turbulent Plume in a Laminar Cross Flow. Atmospheric Environment 6:513-531, 1972.

17. Junod, A., R. J. Hopkirk, D. Schneiter, and D. Hashke. Meteorological Influences of Atmospheric Cooling Systems as Projected in Switzerland. Presented at Symposium on the Cooling Tower Environment University of Maryland, Baltimore. March 4-6, 1974.

18. Keffer, J. F. and W. D. Baines. The Round Turbulent Jet in a Cross Wind. J. Fluid Mech. 15:481-496, 1963.

19. Lee, Jiin. Lagrangian Vapor Plume Model, Version 3. NUS Corporation, Rockville, Maryland. Report No. NUS-TM-5-184. July 1974.

20. Lin, J. T. Three Theoretical Investigations of Turbulent Jets. University of Iowa, Iowa City. Iowa Institute of Hydraulic Research, Report No. 127. January 1971.

21. McVehil, George E. and K. E. Heikes. Cooling Tower Plume Modeling and Drift Measurement, A Review of the State-of-the-Art." Prepared for ASME Contract G-131-1, by Ball Bros. Research Corp., Boulder, Colorado. October 1974 (to be published).

22. Morton, B. R., G. I. Taylor, and J. S. Turner. Turbulent Gravitational Convection from Maintained and Instantaneous Sources. Proc. Roy. Soc. London 234 A, 1 January 1954.

23. Platten, J. L. and J. F. Keffer. Entrainment in Deflected Axisymmetric Jets of Various Angles in the Stream. University of Toronto, Canada. Department of Mechanical Engineering, Report No. UTME-TP0808. 1968.

24. Shirazi, M. A., L. R. Davis, and K. V. Byram. Effects of Ambient Turbulence on Buoyant Jets Discharged into a Flowing Environment. U.S. Environmental Protection Agency, Corvallis, Oregon. Pacific Northwest Environmental Research Laboratory, Working Paper No. 2. June 1974.

25. Slawson, P. R. and G. T. Csanady. On the Mean Path of Buoyant, Bent-over Chimney Plumes. J. Fluid Mech. 28:311-322, 1967.

26. Taft, J. A Numerical Model for the Investigation of Moist Buoyant Cooling Tower Plumes. Systems Science and Software, La Jolla, California. Report No. S55-R-74-2110. February 1974.

27. Taylor, G. I. Dynamics of a Mass of Hotgas Rising in the Air. U.S. Atomic Energy Commission, Los Alamos, New Mexico. Los Alamos Scientific Laboratory, Report No. MDDC-919 (LADC-276). 1945.

28. Turner, D. Bruce. Workbook of Atmospheric Dispersion Estimates. U.S. Public Health Service, Washington, D.C. Publication No. 999 AP-26. Revised 1969.

29. Weil, J. C. The Rise of Moist, Buoyant Plumes. Journal of Applied Meteorology 13:435-441, June 1974.

30. Wigley, T. M. L. and P. R. Slawson. A Comparison of Wet and Dry Bent-over Plumes. Journal of Applied Meteorology 11:335-340, 1972.

31. Wigley, T. M. L. and P. R. Slawson. On the Condensation of Buoyant, Moist, Bent-over Plumes. Journal of Applied Meteorology 10:253-259, April 1971.

SECTION IX

GLOSSARY

A	area
a	vertical acceleration of plume puff
b	local plume radius
C_p	specific heat
DM	entrained incremental mass
d	moisture parameter
e	base of natural logarithm
F	buoyancy flux
F_{it}	buoyancy flux including latent heat
F_{im}	buoyancy flux subtracting liquid moisture
g	gravitational acceleration
H	length of plume segment
L	latent heat of vaporization
l_b	buoyancy scale length
M	mass of plume element
P	pressure
q	mixing ratio
R	gas constant
S	stability parameter
s	distance along plume centerline
T	temperature
T_v	virtual temperature
t	time
U	horizontal velocity component of plume puff
$\underline{V}$	vertical velocity component of plume puff
V	total velocity of plume puff

W	wind velocity
X	horizontal distance
Z	vertical distance
α	shear entrainment coefficient
β	wind impingement coefficient
Γ	lapse rate
ρ	density
σ	liquid water mixing ratio

Subscripts

atm	atmospheric
ad	adiabatic
as	moist adiabatic
ms	maximum, saturated
md	maximum, dry

SECTION X

APPENDICES

APPENDIX A

REVIEW OF PERTINENT PLUME MODELS

There have been several reviews of plume models:

(1) Briggs (2).
(2) The review included in Chan & Kennedy's report (4).
(3) Aynsley and Carson (unpublished) (1).
(4) ASME review (draft, to be published) (21).

This section is not intended to give a complete survey of all past work that has been done, rather it is intended to highlight some of specific past work and point out differences among models.

Present day theories of moist plume behavior rely heavily on previous theories of smoke plume rise and are subject to the same uncertainties. Numerous analytical methods have been proposed. In 1969 Briggs (2) indicated that at the time over 30 models were available.

Much work has been done since then, and several methods have been modified in an effort to account for the effects of moisture. Also, there has been considerable related work in the analysis of submerged buoyant jet discharges in water. Roughly speaking most of the analytical work falls into these categories:

Gaussian Plume Models
Buoyant Plume Models
Numerical Plume Models

GAUSSIAN

Gaussian plume models assume that the concentration of material in a plume cross section has a Gaussian distribution. The rate of growth of the plume cross section as indicated by the rate of increase of the standard deviations of the vertical and horizontal distributions is usually expressed as an exponential function of downwind distance. The usual assumption is that these functions can be related to the turbulent diffusion of the atmosphere which is categorized under different classes of stability. Generally, the Gaussian plume models are used after the plume has assumed to be leveled off. The height of plume rise needs to be determined by other methods.

There are several Gaussian models in the literature. One of the most widely used is incorporated in Turner's Workbook on Atmospheric Dispersion (28). The main difficulty with the Gaussian models is that they do

not model the plume where most of the significant changes occur. However, it is often convenient to use a Gaussian model to solve for the effects of atmospheric diffusion further downwind where the dynamics of the plume are unimportant.

BUOYANT

Buoyant plume rise equations generally have a form similar to the empirical equations obtained by Briggs (2). These can be related to the entrainment concepts suggested by Taylor (27) and Morton, Taylor and Turner (22). Similar derivations are reported by Slawson and Csanady (25) Briggs (2), Hoult (15). Briggs (2) formulations are the simplest:

$$\Delta Z = 1.6\, F^{1/3}\, W^{-1/3}\, X^{2/3} \qquad \text{(neutral conditions)} \qquad (25)$$

$$\text{Maximum } \Delta Z = 2.9 \left(\frac{F}{WS}\right)^{1/3} \qquad \text{(uniform stratification)} \qquad (26)$$

$$\Delta Z = 5.0\, F^{1/4}\, S^{-3/8} \qquad \text{(calm conditions)} \qquad (27)$$

Where:

ΔZ = height of rise
W = wind speed
X = distance downwind
F = buoyancy flux which is proportional to the heat flux
S = stability parameter which is proportional to the potential temperature difference

The coefficients can be shown to be related to the rate at which air is entrained into the plume. Based on entrainment assumptions suggested by Taylor (27) and Morton, Taylor, and Turner (22), similar equations have been derived by Slawson and Csanady (25), Briggs (2), Hoult (15). The formulation used by Hoult for neutral conditions can be written:

$$\Delta Z = \left(\frac{3}{2\beta^2}\right)^{1/3} F^{1/3}\, W^{-1/3}\, X^{2/3} \qquad (28)$$

where:

β = entrainment constant

This is the same as Brigg's relation because the median value of β determined from laboratory tests is reported to be about 0.6 by Fay et al. (10) and Hoult and Weil (16). However, Fay et al. state that field data indicate a higher value for β. They suggest using a value of

$\beta = 0.81$ for the region where the plume is still rising. To find the height to which the plume will rise in a stable stratified atmosphere, they suggest a value of $\beta = 0.55$.

A slightly more general form of the plume rise equation is shown by Hewett, Fay and Hoult (12):

$$\frac{Z}{l_b S}^{2/3} = \left\{ \frac{3}{\beta^2} \left[1-\cos\left(\frac{X}{l_b S}\right)\right]\right\}^{1/3} \tag{29}$$

where

$$l_b \equiv \frac{F}{W^3} \tag{30}$$

The maximum plume rise (the plume oscillates about a mean) is found at $X/l_b S = \pi$, where:

$$\frac{Z_m}{l_b S^{2/3}} = \left(\frac{6}{\beta^2}\right)^{1/3} \tag{31}$$

Fay (1970) gives the rise in the leveled off region as:

$$\frac{Z_\infty}{l_b} = 1.53 \left(\frac{S}{\beta}\right)^{2/3} \qquad \text{at } \frac{X}{l_b S} > 1.55 \tag{32}$$

or

$$\frac{Z_\infty}{l_b} = 2.27 (S)^{2/3} \qquad \text{for } \beta = 0.55 \tag{33}$$

VAPOR PLUMES

There is some disagreement in the scientific literature with regard to predicting the difference in trajectory between dry plumes and vapor plumes. Csanady (6) states that the direct dynamic effects of evaporation and condensation on plume path are minor. His examples show the vapor plume rising only slightly faster than dry plumes. Hosler (14) presents examples where the ultimate height of a vapor plume is several hundred feet lower then that of a comparable dry plume.

Wigley and Slawson (31) make a comparison of wet and dry plumes using essentially the same equation as equation A-5 except that the stability parameter is defined in terms of the moist adiabatic lapse rate rather than the dry adiabatic lapse rate, that is:

$$S = \frac{g}{T_{atm}} (\Gamma_{as} - \Gamma) \tag{34}$$

According to this theory, wet plumes "see" the atmosphere as being more unstable than do dry plumes, and, as a consequence, will rise higher given identical stack parameters (initial temperature excess and efflux velocity) and environmental conditions. Furthermore, if the vapor plume changes between liquid and gaseous phases, it is possible for the "stability" to be different along different parts of the trajectory.

If both moist and dry plumes behave in a stable manner (i.e., $\Gamma > \Gamma_{as}$), the maximum height Z_{ms}, for a condensed plume is related to the maximum height, Z_{md}, for a dry plume:

$$\frac{Z_{ms}}{Z_{md}} = \frac{(\Gamma_{ad} - \Gamma)^{1/2}}{(\Gamma_{as} - \Gamma)^{1/2}} \tag{35}$$

The asymptotic heights of rise will also be in the same ratio. For the case of an isothermal atmosphere:

$$\frac{Z_{ms}}{Z_{md}} \simeq 1.26 \tag{36}$$

Briggs and Hanna (3) argued that Wigley and Slawson's simple replacement of the dry by the moist adiabatic lapse rate was not justified.

Hanna (11) has suggested a simple method for estimating the rise of a moist, buoyant plume in a stable atmosphere. He indicates that if complete condensation of all the initial excess vapor in the plume occurred, then the initial buoyancy flux should include the latent heat released by the excess vapor. The buoyancy flux would then be given by:

$$F_{it} \equiv V_i b_i^2 g \left[\frac{T_v - T_{v_{atm}}}{T_v} + (q_i - q_{atm}) \frac{L}{C_p T}\right] \tag{37}$$

where

T_v = the virtual temperature (T+.61qT)
q = mixing ratio
L = latent heat of vaporization

For a given set of conditions, the ratio of Hanna's moist plume rise to the maximum dry plume rise is:

$$\frac{Z_{ms}}{Z_{md}} = \left(\frac{F_{it}}{F_{id}}\right)^{1/3} \tag{38}$$

This ratio is independent of ambient temperature and humidity stratification. Hanna also gives a second method of calculating plume rise. For this approach, one first calculates the dry plume rise, then computes the fraction of the initial excess vapor that would condense at this height and adds the latent heat released by the condensed vapor to the dry plume buoyancy flux. A new plume is calculated and the procedure iterated until the plume rise converges to a constant value.

Weil (29) has made a comparison of the saturated plume trajectory with the dry plume trajectory for some conditions typical of a large natural draft cooling tower: U_i = 5m/sec, b_i = 30m, ΔT_i = 10° C, Δq_i = .008, $\Delta \sigma_i = 3 \times 10^{-5}$.

where

$\sigma_i \equiv$ mass of liquid water/mass of air

Using Hanna's methodology, and a slightly more approximate form of:

$$F_{it} \equiv V_i b_i^2 g \left[\frac{\Delta T_i}{T_e} + .61\ \Delta q + \frac{L}{C_p T_e}\ \Delta q\right] \tag{39}$$

Weil calculates:

$$\frac{Z_{ms}}{Z_{md}} = 1.44 \text{ (Hanna's first method independent of stratification)}$$

$$\frac{Z_{ms}}{Z_{md}} = 1.30 \text{ (Hanna's second method, } dT_o/dz = 0).$$

$$\frac{Z_{ms}}{Z_{md}} = 2.45 \text{ (Hanna's second method, } dT_o/dz = -.0055° \text{ K/m)}$$

Weil maintains that in the case of a saturated plume in a stable saturated atmosphere, the equations for Z_{ms} and X_{ms} are identical for the dry plume problem. The only real changes are that the definitions of the initial buoyancy flux F_{im} and the stability parameter include the initial vapor (Δq_i) and water ($\Delta \sigma_i$) differences.

That is:

$$F_{im} \equiv V_i b_i^2 g \left(\frac{\Delta T_i}{T_i} + .61\, q_i - \Delta \sigma_i\right) \tag{40}$$

and:

$$S \equiv \frac{d\, g}{T_a} (\Gamma_m - \Gamma) \tag{41}$$

where Γ_m is a reference lapse rate and d is a moisture parameter. Equations for these are given in Weil's paper (29).

Using these definitions and the same initial conditions as before, Weil calculates:

$$\frac{Z_{ms}}{Z_{md}} = 1.18 \qquad \left(\frac{dT_e}{d_z} = 0\right) \tag{42}$$

$$\frac{Z_{ms}}{Z_{md}} = 1.93 \qquad \left(\frac{dT_e}{d_z} = -0.0055 \frac{°K}{m}\right) \tag{43}$$

Note that in the case of an isothermal atmosphere, the method of either Fay, Hanna or Weil predict a maximum moist plume rise roughly 20 to 30 percent higher than the dry plume. However, when the lapse rate was -0.0055 °K/m, Hanna's method predicted moist plume rise almost 2 1/2 times the dry plume rise, while Weil's method predicted about twice the dry plume rise. Unfortunately, the plume trajectories plotted in Figure 3 of Weil's paper can be misleading. Integrating Weil's equations for the 30 meter tower radius listed, results in a dry plume trajectory considerably lower than indicated in the paper. A comparison with Weil's published trajectory is shown in Figure 14. As a check on the solution to Weil's equation, also shown is an independent trajectory obtained from a Lagrangian finite difference model. It compares closely with the numerical solution of Weil's equation. It appears that Weil's trajectories have resulted from considering a point source emission rather than a finite tower diameter.

As discussed above, the difference in the various plume rise estimates are significant. Hopefully field data will lead additional credibility to a given method.

NUMERICAL PLUME MODELS

Several numerical cooling tower plume models have been developed. Unfortunately they are generally proprietary and only brief descriptions are available in the literature. An exception is the EG&G model (8) which was derived under an EPA contract from a cumulus cloud model developed at Penn State by Weinstein and Davis. This model has detailed cloud physics relationships, and the entrainment is assumed inversely proportional to the plume radius. This assumption may be reasonable for a cloud or a nearly leveled off plume puff traveling with the wind, but it is questionable for a plume in a moderately high wind.

The SAUNA (17) computer program appears to be a one dimensional model but a diffusion like spread of matter is assumed to progress downwind from each segment of the plume. This gives rise to a deep "wake" underneath the plume. Some versions use an empirical entrainment mechanism which is more complicated than the EG&G model. An attempt has been made to parameterize a turbulent type of entrainment along with the downwash from the stack.

One of the more sophisticated plume models reported in the literature is that of Systems Science and Software (26). This model calculates a two-dimensional plume cross-section using vorticity relationships, and is able to predict a bifurcation of the plume into two separate parts. However, the horizontal momentum equation is neglected. Entrainment is computed from self-induced "turbulence". The cost of running this proprietary program tends to prohibit its use in prototype design trade-offs.

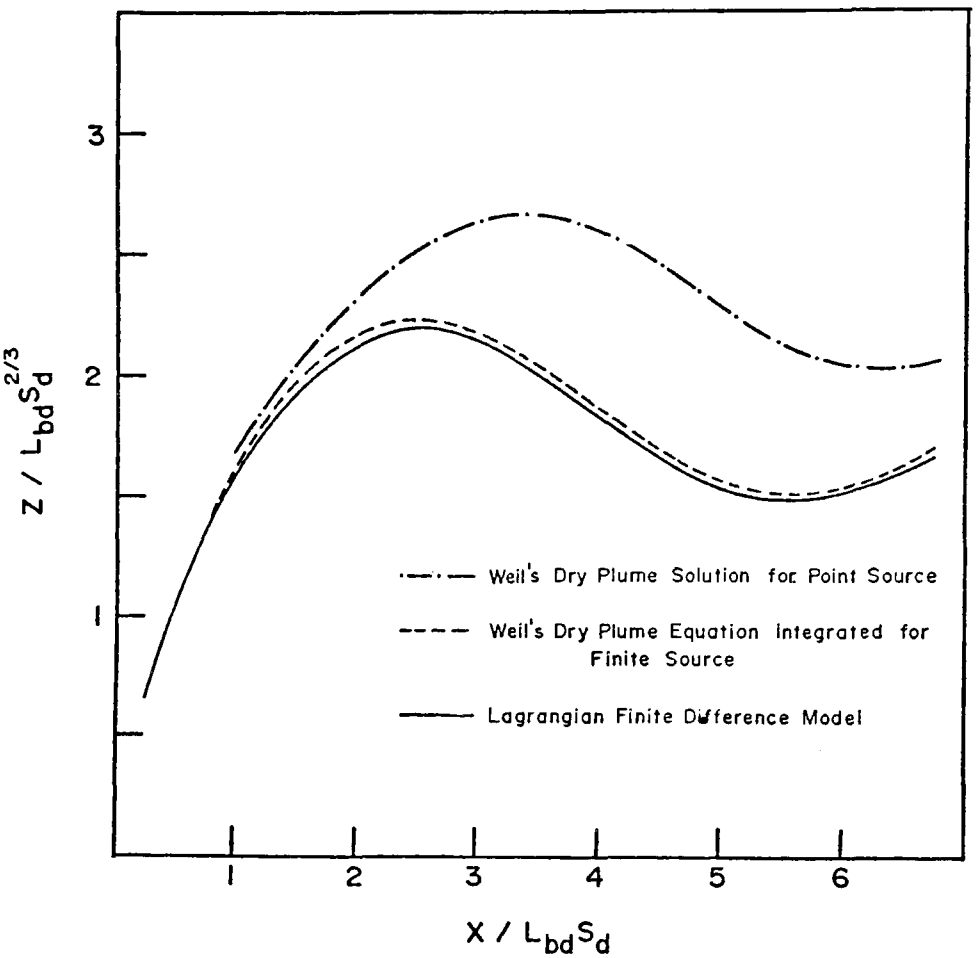

Figure 14 Comparison of Weil's model and the basic Lagragian Puff Model

NUS Corporation has developed a plume model which uses both entrainment and drag terms (19). The drag is calculated like the drag on a solid body. A drag coefficient of 0.3 is used. There may be some ambiguity in the entrainment calculation. Apparently, an entrainment coefficient of 4α is assumed, where α is on the order of 0.1. However, equation 21 of (19) seems to imply that there is no change in volume flux along a stream line. This would mean no entrainment. Unfortunately, complete details about the model are not available, and the effect of this apparent inconsistency is not known. The computational framework of the model is reported to be similar to the Weinstein and Davis cumulus convection model. Both the NUS model and the EG&G model assume a Gaussian dispersion after the maximum plume elevation is reached.

APPENDIX B

MOISTURE COMPUTATION

For sub-saturated conditions moisture is treated as a simple conservative property, i.e.

$$Q_2 = \frac{(Q_1 M + Q_a DM)}{M + DM} \tag{44}$$

Saturation and condensation are encountered when the mixing ratio of the mixed parcel is larger than the saturation mixing ratio for the corresponding temperature. Figure 15 describes the pertinent mechanisms.

Referring to the diagram (Figure 15), the parcel is initially in state (T_1, q_1). (Note: When first saturating (T_1, q_1) may not actually be on the saturation line. However, if the time increments are sufficiently small the error introduced is negligible. Furthermore, after this first step the initial state will be on the saturation curve.) Condensation presumably occurs continuously, equivalently we can suppose that the parcel mixes without condensation and reaches state (T_2, q_2). At this point q_2 is compared to the saturated mixing ratio, q_s, evaluated for T_2. Using the integrated Clausius - Clapeyron equation:

$$q_s = \frac{(6.11)(.622)}{1000} \exp \left[\frac{L}{R_a} \frac{(T_2-273)}{273\ T_2}\right] \tag{45}$$

Since the condensation path slope is nearly horizontal, the temperature rise ΔT caused by condensation can be approximated by:

$$\Delta T = \left[\frac{T_1 - T_a}{q_1 - q_a} -.622 \frac{R_d}{L q_1} \frac{T_1^2}{q_1 + .622} \right] (q_1 - q_2) \tag{46}$$

The change in liquid water mixing ratio is then:

$$\Delta \sigma \simeq \frac{C_p \Delta T}{L} . \tag{47}$$

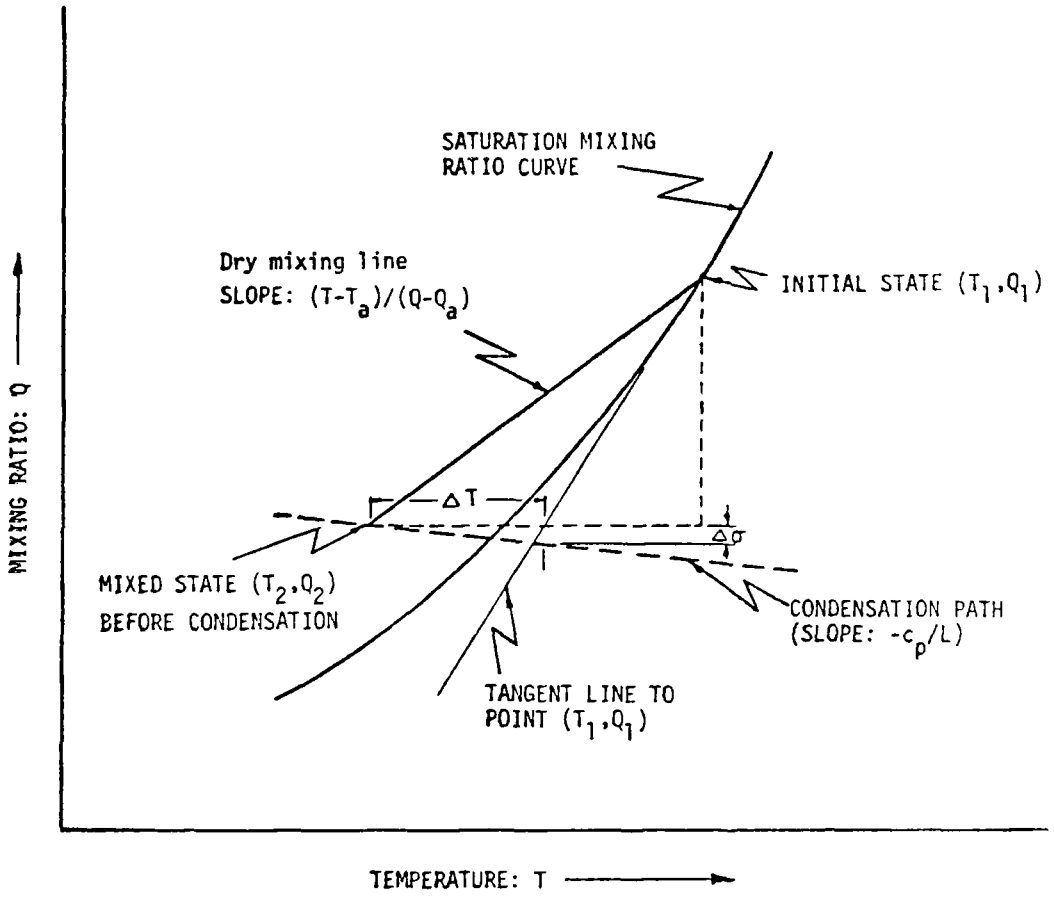

Figure 15 Moisture thermodynamics.

The adjusted amount of liquid water mixing ratio becomes:

$$\sigma \simeq \frac{\sigma_m + \sigma_a \, d_m}{M + d_m} + \Delta\sigma \tag{48}$$

At this point the vapor mixing ratio must be corrected. Simply subtracting $\Delta\sigma$ will, however, lead to iteration errors. Instead the adjusted temperature $T + \Delta T$ is used in the integrated Clausius - Clapeyron equation to find the new mixing ratio. Note then that this method will overestimate the amount of vapor condensed.

If (T_2, q_2) starts to fall below the saturation line, evaporation begins. This mechanism is handled in the same way, except that ΔT and $\Delta\sigma$ become negative.

APPENDIX C

```
      PROGRAM H2OMODEL
      DATA (R=287.),(G=9.8),(TWO=2.),(PI=3.1416) ,(P622=.622),(EL=2500.)
     1,(RV=.461),(T273=273.),(ESO=6.11),(ZERO=0.),(CPD=1.003) ,(DD=1.)
     2,(HHOC=.00525),(ONETHOU=1000.),  (BASET=1.5)
      DO 999 K= 1,12
13    FORMAT(1X,3F7.3,F7.5,4E10.2,F7.2,3F8.4,F7.2,3E8.1)
11    FORMAT (12E9.2,4F6.2)
6     FORMAT (9F8.5,I8)
      READ(60,6)V,UW,T,TA,H,E,A,B,DT,LUL
      IF (EOF(60)) CALL EXIT
      Z= X= TIME=DZ=DB=BSAVE=ZWEI=DH=S =U                          = ZERO
      BA= B
      BO= B*TWO
      WRITE (61,7)
7     FORMAT(" ***********************************************************"/
     1"0    TEMP AM TEMP  HOR VEL  VER VEL      WIND       DIA     THICK*TI
     2ME STEP                                    K  FROUDE                 ")
      VEL= SQRT(U*U+ V*V)
      DENA=ONETHOU-HHOC*(TA-BASET)*(TA-BASET)
      DEN= ONETHOU-HHOC*(T-BASET)*(T-BASET)
      PM= PMO= PI*B*B*H*DEN
      IF ( UW .NE. ZERO) AK= VEL/UW
      FR= VEL/SQRT((DENA-DEN)/DEN*TWO*B*G)
      DT= 1.4/SQRT(VEL*VEL*AK*AK/20. +UW*UW)/1300*AK/10.  /2.
      DTT= DT/100.
      WRITE(61,11 )T,TA,U,V,UW,BO,H,DT,ZERO,ZERO,ZERO,AK,FR
      WRITE (61,8)
8     FORMAT(" -----SUBSEQUENT PLUME VALUES-----"/"      X/D     Z/D     B/
     1D  THICK       MASS  DEL MASS       ZWEI      DEL B    TEMP HOR-VEL VER
     2R-VEL TOT-VEL    S/D                          ")
      ZWEI= ZERO
      LUL= 10000
      DO 99  J= 1, LUL
      EINS= E*DENA*UW*DT*(TWO*B*H*V/VEL+PI*B*DB*U/VEL*H/DD)
      ZWEI= A*DENA*TWO*PI*B*H*DT*ABS(UW*U/VEL-VEL)
      DM= (EINS+ZWEI)*U/UW
      SUM= PM+DM
      U=(PM*U+EINS*UW)/SUM+ZWEI*UW/SUM
      T= (PM*T+ DM*TA)/SUM
      DEN= ONETHOU-HHOC*(T-BASET)*(T-BASET)
      TERM= (EINS+ZWEI)*(UW-U)*U/V/SUM
      IF(U/V .GT.10.) TERM=ZERO
      V=PM*V/SUM+(DENA-DEN)*G/DEN*DT/TWO -TERM
      VI= VEL
      PM= SUM
      VEL= SQRT(U*U+ V*V)
      DZ= V*DT
      DX= U*DT
```

```
      DD= VEL*DT
      BSAVE= B
      B= SQRT(PM/(DEN*PI*H))
      DB= (B-BSAVE)
      DH= (VEL-V1)/DD*H*DT
      H= H+ DH
      X= X+ DX
      Z= Z+DZ
      DT= DT+DTT
      IF (J .EQ. 1) GO TO 98
      IF(J/200-(J-1)/200 .NE. 1) GO TO 99
      IF (RATIOZ .GT. 40. .OR. RATIOX .GT. 100.) GO TO 999
98    RATIOX= X/B0
      RATIOZ= Z/B0
      RATIOR= B/BA
      WRITE(61,13) RATIOX,RATIOZ,RATIOR,H,PM,DM,ZWEI ,DB,T,U,V,VEL
99    CONTINUE
999   CONTINUE
      CALL EXIT
      END
```

```
      PROGRAM AIRMODEL
      DATA (R=287.),(G=9.8),(TWO=2.),(PI=3.1416) ,(P622=.622),(EL=2500.)
     1,(RV=.461),(T273=273.),(ESO=6.11),(ZERO=0.),(CPD=1.003)
     2,(ADIA=.0098),(ONE=1.), (SIXI=.61)
11    FORMAT (2F7.1,3F7.2,2E10.2,4F7.4,2F7.2,2F8.4,2F7.3)
13    FORMAT(1X,3F7.3,F7.5,4E10.2,F7.2,3F8.4,F7.2,F8.6,2E8.1)
      DO 999 KAY= 1,5
6     FORMAT (9F8.5,I8)
      READ(60,6) V,UW,T,TA,H,A,E,B,DT,LUL
      IF (EOF(60)) CALL EXIT
      READ (60,6) U,DTO,Q,QA, SIG ,SIGA ,P,DUW
      READ (60,6) DESIRED1,DESIRED2
      Q     =  ESO  *EXP(EL/RV*((T-T273)/T273/T))/1000. *P622
      AK= SQRT(V*V+U*U)/UW
      DEN =P/R/T /(ONE+SIXI*Q )*(ONE+SIG)
      DENA=P/R/TA/(ONE+SIXI*QA)*(ONE+SIGA)
      FR= V/SQRT((DENA-DEN)/DEN*TWO*B*G)
      DT= ONE/SQRT(VEL*VEL*AK*AK/29.+UW*UW) *AK/200.
      DTT= DT/30.
      Z= X= DZ=S                                          =ZERO
      BA= B
      BO= B*TWO
      A= .057
      WRITE (61,7)
7     FORMAT(" ***********************************************************"/
     1"0        T      TA       U        V      UW       B          H          DT
     2   SIG    SIGA      QA       Q       K      FR      DTO      DUW        A
     3    E")
      WRITE(61,11 )T,TA,U,V,UW,B ,H,DT,SIG,SIGA,QA,Q,AK,FR,DTO,DUW,A,E
      WRITE (61,8)
8     FORMAT(" -----SUBSEQUENT PLUME VALUES-----"/"      X/D     Z/D     B/
     1D  THICK       MASS  DEL MASS       ZWEI      DEL B   TEMP HOR-VEL VER
     2R-VEL TOT-VEL    S/D  MIX R. LIQ HHO      ")
      VEL= SQRT(U*U+ V*V)
      PM= PI*B*B*H*DEN
      DO 99 J= 1,LUL
      UW= UW+ DUW*DZ
      TA= TA- DTO*DZ
      DP= -DENA*G*DZ
      P= P+DP
      EINS= E*DENA*UW*DT*(TWO*B*H*V/VEL+PI    *B*DB*U/VEL*H/DD)
      ZWEI= A*DENA*TWO*PI*B*H*DT*ABS(UW*U/VEL-VEL)
      DM= (EINS+ZWEI)*U/UW
      SUM= PM+DM
      U= (PM*U+EINS*UW)/SUM+ ZWEI*UW/SUM
      QSS   =  ESO  *EXP(EL/RV*((T-T273)/T273/T))/1000. *P622
      TS= T
      T= (PM*T+ DM*TA)/SUM -ADIA*DZ
      QS1   =  ESO  *EXP(EL/RV*((T-T273)/T273/T))/1000. *P622
      Q= (Q*PM+QA*DM)/SUM
      IF (Q .GT. QS1 .OR.  SIG .GT. ZERO) GO TO 110
      GO TO 111
110   DTEM= ((T-TA)/(Q-QA)-P622*RV*(T+TS)*(T+TS)/4./QS1/EL/(QSS+P622))*(
     1QSS-Q)
```

```
      DSIG= DTEM*CPD/EL
      T= T+ DTEM
      SIG= (SIG*PM +SIGA*DM)/SUM + DSIG
      IF (SIG. LT. ZERO) SIG= ZERO
      Q      =  ESO  *EXP(EL/RV*((T-T273)/T273/T))/1000. *P622
111   CONTINUE
      DENA=P/R/TA/(ONE+SIXI*QA)*(ONE+SIGA)
      DEN =P/R/T /(ONE+SIXI*Q )*(ONE+SIG)
      TERM= (EINS+ZWEI)*(UW-U)*U/V/SUM
      IF (U/V .GT. 10.) TERM= ZERO
      V= (PM*V      )/SUM         +(DENA-DEN)*G/DEN*DT/TWO -TERM
      PM= SUM
      V1= VEL
      VEL= SQRT(U*U+ V*V)
      DZ= V*DT
      DX= U*DT
      DD= SQRT(DZ*DZ+ DX*DX)
      H= H+ (VEL-V1)/DD*H*DT
      BSAVE= B
      B= SQRT(PM/(DEN*PI*H))
      DB= B-BSAVE
      DT= DT+ DTT
      X= X+ DX
      Z= Z+DZ
      S= S+ DD
      IF (J .LE. 2) GO TO 98
      IF (X .GT. DESIRED1 .AND. X .LT. DESIRED2) GO TO 98
      IF (J/150 -(J-1)/150 .NE. 1) GO TO 99
98    RATIOZ= Z/B0
      RATIOS= S/B0
      RATIOR= B/BA
      RATIOX= X/B0
      WRITE(61,13) X,Z,          RATIOR,H,PM,DM,ZWEI ,DB,T,U,V,VEL
     1,RATIOS,Q,SIG
99    CONTINUE
999   CONTINUE
      CALL EXIT
      END
```

APPENDIX D

ENTRAINMENT COMPUTATION

The total entrainment (impingement + aspiration) is computed such that the horizontal momentum flux of the entrained mass plus the assumed pressure force equals the sum of the horizontal momentum of the wind impinging on the projected area plus the horizontal momentum that the aspirated wind mass carries with itself.

$$\underbrace{(\text{entrainment})\ W}_{\substack{\text{horizontal momentum flux of the entrained fluid}}} + \underbrace{(\rho A_p W + \text{aspiration})\ (W-U)}_{\substack{\text{pressure force assumption}}}$$

$$= \underbrace{\rho A_p W^2 + (\text{aspiration})\ W}_{\substack{\text{total horizontal momentum flux assumed to be available}}} \qquad (49)$$

therefore:

$$\text{entrainment} = (\rho A_p W + \text{aspiration})\ \frac{U}{W} \qquad (50)$$

TECHNICAL REPORT DATA
(Please read Instructions on the reverse before completing)

1. REPORT NO.	2.	3. RECIPIENT'S ACCESSION NO.
EPA-600/3-76-100		

4. TITLE AND SUBTITLE	5. REPORT DATE
Cooling Tower Plume Model	September 1976
	6. PERFORMING ORGANIZATION CODE

7. AUTHOR(S)	8. PERFORMING ORGANIZATION REPORT NO.
Lawrence D. Winiarski and Walter E. Frick	

9. PERFORMING ORGANIZATION NAME AND ADDRESS	10. PROGRAM ELEMENT NO.
Assessment and Criteria Development Division Corvallis Environmental Research Lab 200 SW 35th Street Corvallis, Oregon 97330	EHE252
	11. CONTRACT/GRANT NO.

12. SPONSORING AGENCY NAME AND ADDRESS	13. TYPE OF REPORT AND PERIOD COVERED
U.S. Environmental Protection Agency Corvallis Environmental Research Center Corvallis, Oregon 97330	in-house
	14. SPONSORING AGENCY CODE EPA/ORD

15. SUPPLEMENTARY NOTES

16. ABSTRACT

A review of recently reported cooling tower plume models yields none that is universally accepted. The entrainment and drag mechanisms and the effect of moisture on the plume trajectory are phenomena which are treated differently by various investigators. In order to better understand these phenomena, a simple numerical scheme is developed which can readily be used to evaluate different entrainment and drag assumptions. Preliminary results indicate that in moderate winds most of the entrainment due to wind can be accounted for by the direct impingement of the wind on the plume path. Initially, the pressure difference across the plume is found to produce a substantial drag force. Thus, it is likely that a certain portion of the plume bending is due to these pressure forces, and artificially increasing wind entrainment to fit experimental data is unnecessary.

17. KEY WORDS AND DOCUMENT ANALYSIS

a. DESCRIPTORS	b. IDENTIFIERS/OPEN ENDED TERMS	c. COSATI Field/Group
coolint towers, plumes plume computer programs plumes trajectories plumes cooling towers plumes, thermal analysis plumes, atmospheric diffusion		Field 14 group 131+

18. DISTRIBUTION STATEMENT	19. SECURITY CLASS *(This Report)*	21. NO. OF PAGES
Release unlimited	unclassified	72
	20. SECURITY CLASS *(This page)*	22. PRICE
	unclassified	

EPA Form 2220-1 (9-73)

☆ U. S. GOVERNMENT PRINTING OFFICE: 1976—698-028/129 REGION 10